EARTH SCIENCES CENTRE
GÖTEBORG UNIVERSITY
A61 2000

MODELING FJORD CIRCULATION AND TURBULENT MIXING

Olof Liungman

Department of Oceanography
GÖTEBORG 2000

Modeling fjord circulation and turbulent mixing

Olof Liungman

Department of Oceanography
Göteborg University
Göteborg, Sweden
A61/2000, ISSN 1400-3813

Printed in Sweden
Kompendiet-Göteborg
2000

Abstract

This thesis deals with circulation in sill fjords and turbulent mixing, with a focus on numerical modeling. The major topics are net circulation in an open-ended system, turbulent entrainment into dense overflows, deep-water turbulent diffusion and turbulence closure schemes. Special reference is made to a system of fjords on the Swedish west coast.

The focus on sill fjords is motivated by the wide spectrum of oceanographic processes occurring in these coastal inlets. Because of restricted exchange with exterior water masses, coupled with local river input, fjords exhibit large spatial gradients in hydrographic and biochemical properties. The deep basin water is subject to renewals and stagnation. Renewals are a result of inflows caused by coastal upwellings, and tend to be episodic events dominated by advective processes and entrainment. Between renewals the deep water is trapped behind the sill, causing stagnation, during which only interior turbulent mixing can affect the deep water properties.

The thesis is based on four papers. Paper I deals with an open-ended Swedish fjord system. Direct and indirect current measurements are presented which indicate a net through-flow in a counterclockwise direction. Using long-term hydrographic observations and a process-oriented box model it is shown that the throughflow is primarily forced by the along-coast steric height difference between the ends of the fjord system. Though density driven currents through the deeper entrance dominate the exchange at large, periods of reversing net flow may significantly influence the northern basins. In Paper II a specific renewal event in a small Swedish sill fjord is investigated, with focus on the entrainment of resident water by inflowing juvenile water and its parameterization. A 1-D numerical model is used together with observations to show the large impact of entrainment on the post-renewal state of the fjord. The likely effect of this mixing on the occurrence of subsequent renewals is emphasized. The subject of Paper III is weak turbulent mixing in stagnant fjord basin. A model is proposed in which the internal wave energy, generated by the interaction of the barotropic tide with the sill topography, is added as a source term in the equation for the turbulent kinetic energy in a second-order turbulence closure scheme. The model is shown to agree with observations in two Scandinavian fjords. Finally, in Paper IV an alternative parameterization of the turbulent length scale, as well as a modification of the stability functions used in second-order turbulence closure schemes, are proposed. The resulting one-equation eddy viscosity model, to be used in geophysical applications, is validated against a number of data sets and compared to the k-ε model.

Keywords: fjord circulation, steric height, deep water renewal, stagnation, bottom plume entrainment, turbulence modeling, internal wave mixing, turbulent length scale, stability functions

Table of contents

Appended papers

Paper I. Björk, G., O. Liungman, and L. Rydberg, 2000: Net circulation and salinity variations in an open-ended Swedish fjord system. *Estuaries*, **23**, 367-380.

Paper II. Liungman, O., L. Rydberg, and C.-G. Göransson, 2000: Modeling and observations of deep water renewal and entrainment in a Swedish sill fjord. *Submitted to Journal of Physical Oceanography.*

Paper III. Liungman, O., 2000: Tidally forced internal wave mixing in a k-ε model framework applied to fjord basins. *Journal of Physical Oceanography*, **30**, 352-368.

Paper IV. Axell, L. B., and O. Liungman, 2000: A one-equation turbulence model for geophysical applications: comparison with data and the k-ε model. *Submitted to Environmental Fluid Mechanics.*

"There are no fish in my computer."

Remark made by the author during an interview for radio when the interviewer — having received the answer "oceanographer" when inquiring the author's profession — enthusiastically began talking about how he sometimes dreamt he was a dolphin...

1 Introduction

What this thesis is all about and why

The work summarized in this thesis deals with two separate subjects that nevertheless are intimately connected: fjords and turbulence. The first is a large geographical feature, the second a small-scale process. Why these particular choices? Well, in a way it was a matter of chance. My supervisor Lars Rydberg, whom I had assisted on another project, wanted to take a closer look at the Orust-Tjörn fjord system. He approached me and I, having at the time recently graduated, was enormously interested in anything that involved earning a salary... On the other hand, fjord oceanography has been a subject of study at the Department of Oceanography in Göteborg ever since the days of Otto and Hans Petterson in the early 20th century, and their work at the Bornö Station in Gullmarsfjorden. This tradition has been carried on by Nils Zeilon, Börje Kullenberg and currently Anders Stigebrandt. It is interesting to note that a so-called Extended Essay, which I wrote at the age of 18, was actually entitled *Fjord Oceanography*. So perhaps fate was involved a little, too.

As for turbulence, this is a very interesting topic, not only to those of us studying the oceans. Turbulence has an absolutely vital impact on all kinds of fluid flows, despite the small scales it acts on. From water pipes to weather systems, turbulence determines the mixing. When you as an oceanographer try to improve your understanding of how the oceans work, you usually end up making clever guesses about the rate and distribution of mixing. Thus, turbulence is a key issue if we are to gain greater insight into the dynamics of the oceans.

Though a great deal of work has been done on turbulence during the last 100 years or so, it is still one of the more important unsolved problems in physics. Furthermore, from an oceanographic point of view, results based on painstaking laboratory investigations do not always apply all that well out in the oceans. This is where fjords re-enter the picture. Fjords are probably the closest an

oceanographer will ever come to a life-sized laboratory experiment, where there is some chance of separating between different processes as well as quantifying them with reasonable accuracy. Fjords are small compared to oceans, relatively easy to access and sample, and with restricted, measurable exchange with the surroundings. At the same time they are of geophysical dimensions and exhibit many of the properties and features of a large ocean.

So, what about the term "modeling" in the title? As will be discussed later in this thesis, to model is to describe a physical process in mathematical terms, enabling you to perform calculations and (hopefully) make predictions. Oceanographers tend to discern between those who do mostly theoretical work, those who concentrate on making measurements in the laboratory or at sea, and those who do computer modeling. The latter are commonly referred to as modelers. I was once asked at a conference dinner what "kind" of oceanographer I was. I had no idea what to answer but was rescued by my colleague and friend Bo Gustafsson, who immediately answered "modeler". Though I have taken part in several field programs and struggled through a great deal of turbulence theory, my main interest has always been to attempt to recreate the reality revealed through observations using computer simulations. Why? Basically because it is fun and interesting, but also because (i) it is a way of testing our ideas about how things work, and (ii) it is important to be able to calculate possible outcomes of changes in nature. The latter is true not only when considering such matters as a possible global warming, but also on much smaller scales, for example, the environmental impact of lengthening a harbour pier, problems of a kind that I and my colleagues at the Swedish Meteorological and Hydrological Institute (SMHI) encounter on an almost daily basis.

What this thesis contains

This thesis is based on four papers, all of which may be found in the back. Two I have put under the heading *Fjord circulation*, because they deal with specific features of water circulation and exchange

in fjords or systems of fjords. The other two papers go under the heading *Turbulent mixing*. The first of these papers (Paper III) also concerns fjords, namely weak turbulent diffusion in the deep water of stagnant fjords. The fourth paper I have put last because it does not explicitly deal with fjords, though the model it describes is perfectly applicable to fjords. I've tried it.

The booklet you are holding is what we call a "compilation thesis", that is it consists of published or submitted papers preceded by what I will refer to as the preamble. The purpose of the preamble is to introduce the separate papers, put them into context and perhaps to add such results and thoughts that did not fit in the papers.

Here, I would like to emphasize the following. I have chosen, on my own, to write this preamble in such a way that a marine scientist from another discipline, and perhaps even a layman, should be able to follow most of it. Hence, I have kept equations to a minimum and I have tried to focus on concepts instead of details, using simple everyday terms. For someone with extensive knowledge of physical oceanography this may at times seem too simplistic. If you want the hard facts and nitty-gritty details, please read the papers.

There are many reasons why I chose to write the preamble in the way I did. As a scientist one is repeatedly told how important it is to spread one's results to the general public. Also, I have learned and re-learned a great deal, while trying to put into simple words something that I and my fellow oceanographers take for granted. Finally, I nurture a slim hope that because of the way I have chosen to write the preamble, this thesis will perhaps be read by someone else but myself, my supervisors and my examiners...

Thanks are due...

A great number of people have contributed in one way or another to the making of this thesis. Should I put them all in here this would turn into a very long introduction. Nevertheless, there are some which I perhaps may not get to thank enough, and which I therefore would like to mention here.

Let me begin with my team of supervisors, who kept me from heading off in all the wrong directions: Lars Rydberg, Göran Björk and Gösta Walin. Though not my supervisor, Anders Stigebrandt deserves to be mentioned as many of my ideas are based on his earlier work and helpful suggestions. Many thanks also to my colleagues at the Department of Oceanography who put up with a fellow researcher who apparently cannot think without talking to someone. Among these I want to include our fellow oceanographers in Stockholm, particularly Tim Fristedt who made our studies together great fun. Thank you, all of you, for all the good times, at work and elsewhere. Since this thesis was completed during a few hectic weeks in San Francisco, California, I must not forget to mention J.B. and Tuula Delaney, who helped me and my wife upon our arrival in the States and who lent me their laptop computer when mine broke down! I would also like to thank Lars Axell for the fun we have had working together, Anders Omstedt for his optimism, Urban Svensson for teaching me about turbulence modeling and C-G Göransson for helping out and for being so enthusiastic. At SMHI, I must mention my friends and colleagues at the oceanographic consulting group, who have put up with my short, infrequent visits at work and always supported my efforts to earn a Ph.D. I hope to spend more time with you soon. Many thanks also to my dear friend Michael Rodahl, whose thesis has been something of a template for this one, and whose appropriate but sometimes brutally realistic comments have kept me from wandering off from time to time, particularly in view of my sometimes too optimistic time tables. Last but definitely not least, my wife Cecilia Hartman and our respective families for all the years of support. I needed it.

Let me conclude this introduction by paraphrasing a rather famous traveller:

> A small stumble for mankind, a five-year roller coaster for me.

2 Fjord circulation

The major subject of my thesis, and which I will focus on in this chapter, is the circulation of water in a particular type of coastal features called fjords. In Merriam-Webster's Collegiate Online Dictionary, the entry for fjord reads:

> "Fjord — Norwegian *fjord*, from Old Norse *fjorthr*: a narrow inlet of the sea between cliffs or steep slopes."

This definition, however, focuses on what is above water and does not really catch what makes fjords interesting to an oceanographer, namely the restricted circulation. Kjerfve and Magill (1989) define a fjord as:

> "A glacially scoured inland marine area with sea water measurably diluted by land drainage in the surface layer, consisting of high-salinity waters in deep basins, affected by tides, and usually measuring several hundred meters in depth."

In this definition, the most important characteristics of fjords are emphasized, namely the co-existence of different water masses (surface and deep basin water) and the influence of both coastal processes (land drainage) and open sea processes (tides).

2.1 An introduction to fjord oceanography

General description of fjords

Fjords are only found at higher latitudes in previously glaciated areas: Scandinavia, Iceland, Spitzbergen, Greenland, Antarctica, southern New Zealand, west coasts of Canada, Alaska and Scotland, and southern Chile. They are in general, as stated in the definition above, the result of glacial erosion, often along fissures or other zones of weakness in the bedrock. Many fjords have narrow

openings towards the sea. As a result exchange with exterior water masses may be severely limited. Hence, the properties of the interior water masses are likely to be quite different from those of the exterior, which would not be the case if the exchange was large at all times. Instead, the hydrography of the fjord, that is, its salinity and temperature and the changes in these parameters, is affected by several different processes such as freshwater supply, heat exchange with the atmosphere, solar irradiation, deep water diffusion and episodic deep water renewals or overflows due to coastal upwellings[1] (see, e.g., Farmer and Freeland 1983). In fact, fjords can be seen as miniature oceans, with to some degree their own ecology and specific hydrographic properties. To compare the circulation in Byfjorden or Oslofjord to that of the Baltic Sea or even the Pacific Ocean, is not as incredulous as it may sound. To some degree the same processes control the state of all these basins, and in some cases it can be worthwhile to utilize the concept of a semi-enclosed estuary even for oceans (Stigebrandt 1984). To summarize, it is the complex interplay between exterior and interior processes which determines the hydrographic state of a fjord. This is what Papers I and II are all about and will be the subject of the present chapter.

Sill fjords

A sill fjord is a fjord where the mouth is shallower than the fjord basin. This shallow part is called the sill and may be the result of decreased erosion near the end of a glacier, or a terminal moraine. A schematic of the basic features of a sill fjord, as well as the important processes affecting the hydrographic state, is shown in Figure 1. The waters above the sill commonly experience a fairly large exchange with the sea outside. This surface water exchange may be due to estuarine circulation[2], tidal currents and intermediary flows

1. This is when dense water usually found at greater depths rises to near the surface at a coast.

caused by horizontal density gradients (see, e.g., Stigebrandt 1980, 1981, 1990; Farmer and Freeland 1983). The shallow sill implies that the deep basin (below sill depth) is more *or less cut off* from the water masses outside. Only if the water entering over the sill is denser, and thus heavier, than that in the deep basin can the inflowing water penetrate to the deeper parts of the basin, replace the deep water and cause a *renewal* (see, e.g., Gade and Edwards 1980). Otherwise the deep basin water is said to be *stagnant*, and only mixing by interior turbulent mixing[3], or possibly convective events, can affect its properties. If the stagnation periods are long enough (on the order of months or years) all the available deep water oxygen may be used up through biological respiration. Reduced oxygen levels, and eventually oxygen deficit, results in a quite different hydrochemistry in deep waters and bottoms, which may involve production of hydrogen sulfide by anaerobic bacteria. The biochemical processes as such are beyond the scope of this thesis, though of course of great general

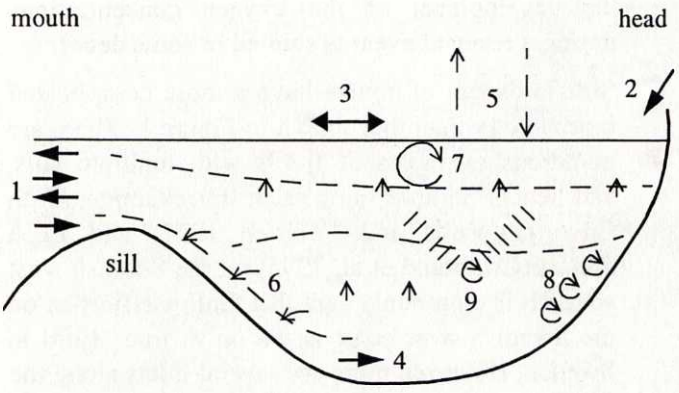

Figure 1. A schematic illustrating some of the different processes taking place in a fjord. Dashed lines show regions of strong changes in density, pycnoclines. The numbers refer to: (1) sill exchange, (2) river input, (3) wind, (4) deep water inflow, (5) atmospheric exchange, (6) bottom plume entrainment, (7) wind mixing, (8) mixing by breaking internal tide, and (9) mixing by interacting internal waves.

2. This is the outflow of surface water made brackish by river input and the simultaneous inflow of intermediary, more saline water.

3. Deep water mixing in fjords will be discussed in detail in chapter 3.

interest to fjord oceanographers. It is also obvious that the physics involved in the exchange of deep water in fjords is of utmost importance to the hydrochemistry. This is addressed in Paper II where the development of the oxygen concentrations during a renewal event is studied in some detail.

Systems of fjords

Sill fjords can of course have a more complicated morphology than that shown in Figure 1. There are numerous examples of fjords with multiple sills, and hence multiple fjord basin, for example, Loch Etive (Edwards and Edelsten 1977) and Loch Sunart (Gillibrand et al. 1995) on the Scottish west coast. It is commonly said that Gullmarsfjorden on the Swedish west coast is the only "true" fjord in Sweden. However, there are several inlets along the Swedish west coast which for all practical purposes may be termed fjords. An interesting area is the system of fjords inside the islands of Orust and Tjörn, shown in Figure 2, which consists of a number of basins separated by constrictions and sills. Surrounding coastal areas, between Marstrand and Lysekil, are fairly densely populated with several large industries located along the shores of the fjords. In addition to serving as a recreational area, there is also extensive commercial mussel farming in the fjords (Haamer 1995). What makes this fjord system particularly interesting to oceanographers is the existence of two openings towards the Skagerrak, which allows for a net one-way flow through the system. This issue, together with other processes controlling the properties and circulation of the water above sill depth in the Orust-Tjörn fjord system, is the subject of Paper I.

Deep water renewal

As described earlier, sill fjords go through a cycle of stagnation and renewal. The stagnation periods are interrupted by renewal events, when the *resident*, stagnant deep basin water is replaced by *juvenile*, more dense (and thus heavier) water from the outside. The inflowing water will change the hydrographic properties of the deep basin, increasing the salinity (and therefore the density) and most likely the oxygen concentrations as well. This process involves the inflow of dense water

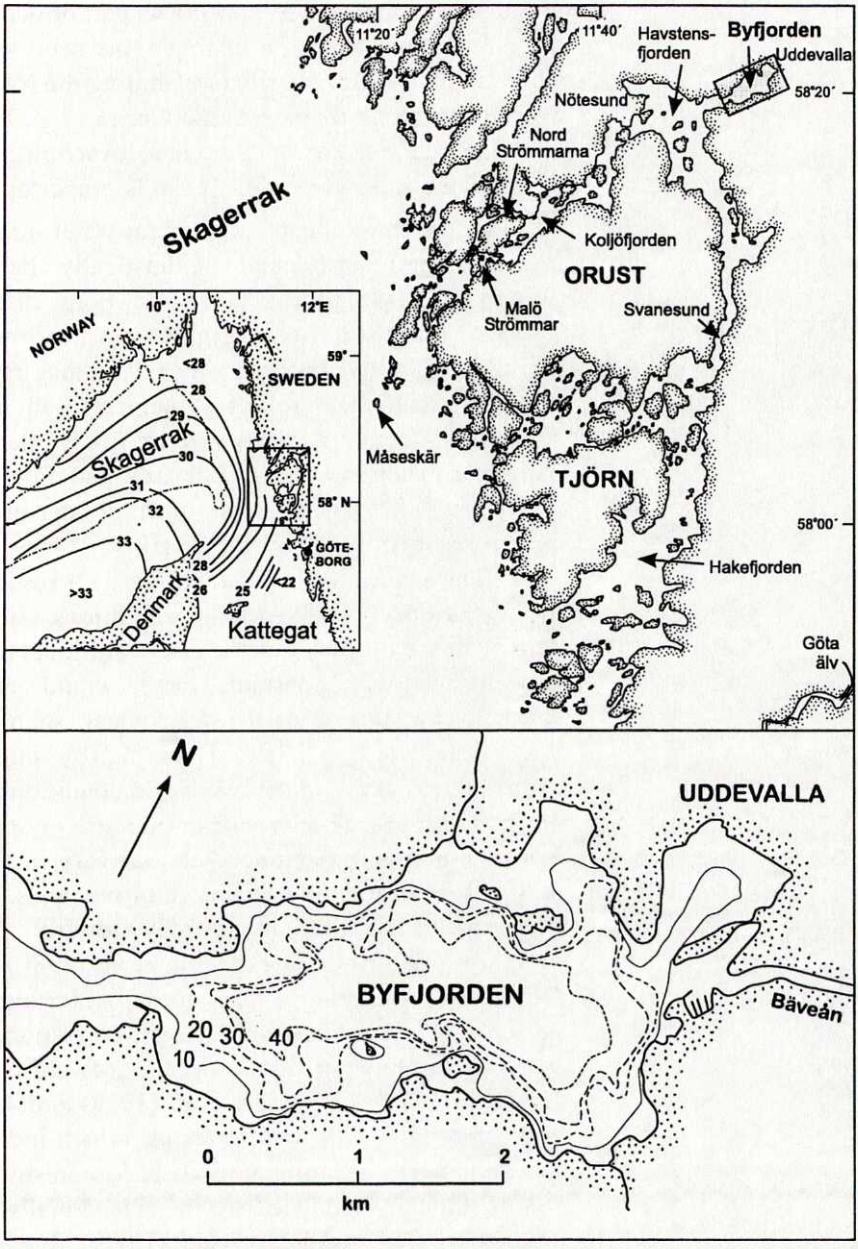

Figure 2. A map showing the Orust-Tjörn fjord system and its location on the Swedish west coast, as well as a detail of Byfjorden. The inset also shows the mean surface salinity field in the Skagerrak and northern Kattegat May-August (from Rodhe 1996).

over the sill, which will form a dense bottom plume that flows down-slope to the deeper parts of the fjord basin (Gade and Edwards 1980). Such a process, though on a much smaller scale, is similar

to the oceanic overflows ocurring as part of oceanic deep water formation, for example, the deep water flows across the bottom ridge separating the Nordic Seas from the northern Atlantic Ocean (e.g., Price and Yang 1998). For both oceanic overflows and deep water inflows in fjords, it is important to consider the entrainment[4] of ambient water into the bottom plume. Entrainment can drastically alter the properties of the plume as, in the fjord case, it implies extensive mixing between inflowing juvenile water and resident water. It is thus rather surprising that this process is neglected in most studies of deep water renewal in fjords, though there are exceptions (e.g., Edwards and Edelsten 1977). I will discuss this topic in detail later in this chapter, as it is the focus of Pape rII.

The intermittency of renewals is a result of the variations in the exterior conditions. If the density of the inflowing water above sill level in the sea outside was constant, there would be a continuous exchange of the deep water, such that deep water inflow balanced mixing by interior diffusion. However, in the real world conditions are never constant. Winds, tides, pressure systems, coastal currents, river runoff, etc. all vary in time, and will influence the occurrence of renewals. The time scale of this intermittency may vary from days to years. The results of Edwards et al. (1980) and Geyer and Cannon (1982) show a fortnightly periodicity in bottom water inflows, corresponding to the spring-neap tidal cycle. Edwards and Edelsten (1977), Gillibrand et al. (1995) and Allen and Simpson (1998) present results which indicate that inflows occur during periods of low freshwater runoff, though modulated by the tide. Finally, the studies by, for example, Gade (1973), Svensson (1980) and myself (Paper III) describe stagnation periods of several years.

Of course, no renewal will occur unless there is an adequate supply of water of sufficiently high

4. This is the process of mixing across the interface between two flows with different velocities.

density above sill level outside the fjord mouth, as discussed by, for example, Gade and Edwards (1980). Hence, though inner processes are necessary to predispose a fjord for renewal, the actual time of occurrence is in general determined by exterior processes (e.g., Cannon et al. 1990).

Though a great deal of work has been done in attempting to deduce why renewals occur, studies of the details of a renewal event are much less common. The reason is of course that since renewals are rare and episodic events, they are also difficult to predict and observe. However, some attempts have been made. Edwards and Edelsten (1977) and Edelsten et al. (1980) analyze two renewal events, in Loch Etive and Loch Eil respectively, and estimate the entrainment into a dense bottom plume from current measurements. Based on a combination of current, temperature and salinity measurements Allen and Simpson (1998) describe several renewal events in Upper Loch Linnhe, as well as the two-dimensional circulation during one of the events.

In Paper II, my co-authors and I attempt to separate the different processes taking place during a particularly strong renewal event in Byfjorden, the innermost appendix of the Orust-Tjörn fjord system, that occurred in April and May of 1974. Using observations together with a one-dimensional numerical model[5], we focus on the sill flow and the mixing of resident and inflowing water through entrainment. We also present a comparison between different entrainment formulae and show the importance of the entrainment in determining the post-renewal state of the fjord.

---

5. A one-dimensional model is where the properties being modeled are assumed to vary in only one of the three spatial dimensions, in our case vertically. In addition, a one-dimensional model can be either stationary (no variations in time) or non-stationary (time dependent). Numerical, in this context, means using a computer to determine an approximate solution that satisfies the model equations in a finite number of points in time and space.

2.2 The subtidal circulation above sill level in an open-ended fjord system

The issue

The Orust-Tjörn fjord system is located where the Kattegat, strongly influenced by the low-saline Baltic outflow (20-30 psu; Andersson and Rydberg 1988), meets the Skagerrak of almost oceanic salinities (32-35 psu; Rydberg et al. 1996). The two meet at the Kattegat-Skagerrak front, which in general stretches northeastwards from Skagen in Denmark towards the Swedish coast (e.g., Gustafsson and Stigebrandt 1996). Observations compiled by Rodhe (1996) indicate a maximum in the variability of the surface salinity just outside the fjord system. This implies that the largest horizontal salinity gradient, or in other words the largest change in salinity going northward along the coast, is found in this area (see Figure 2). To the north, salinities are higher and to the south they are lower.

As described in the previous section, the Orust-Tjörn fjord system is open to the sea at both its northern and southern end. Two separate investigations have indicated the existence of a counterclockwise net throughflow in the system, that is, in through the southern entrance and out through the northern (Ehlin 1971; U. Cederlöf and L. Djurfeldt, personal communication). I should mention that the word *net* is connected to the word *subtidal* in the heading of this section. There is constantly a flow back and forth through the fjord system due to the primarily semi-diurnal tide. Twice a day[6] there is a flow into the fjord system, and twice a day there is a flow out. However, averaging over a sufficiently long time period will filter out the tidal fluctuations and we are left with long-term net flows. Variations in these net flows will occur on much lower frequencies than those dominating the tide, that is on subtidal frequencies.

6. To be more precise, during two six-hour periods every day.

Until recently no clear explanation of the forcing behind such a net flow had been presented. It is natural to consider the along-coast density gradient described earlier as a prime candidate for driving a net flow through the fjord system. Heavy water from the north will want to flow southward below the lighter water in the south, which will want to move in the opposite direction. However, the northern entrances to the fjord system, Malö Strömmar and Nordströmmarna (see Figure 2), are very shallow — less than 10 m — and there are no indications of a stratified flow. Obviously, things are a little more complicated than the simple picture presented here. To continue, I will have to introduce the concept of steric height.

Steric height

The steric height h_s is defined as the vertical distance between two surfaces of constant pressure (isobars) and is given by

$$h_s(z_1, z_2) = \int_{z_1}^{z_2} \frac{\Delta\rho}{\rho_0} dz, \qquad (1)$$

where $\Delta\rho=\rho_0-\rho(S,T)$ is the difference between the density ρ at a given depth and a suitable reference density ρ_0 (Tomczak & Godfrey 1994). Note that I have neglected the effect of pressure on the density. Equation (1) shows that the less dense the water, the longer the vertical distance between two isobars. If we can neglect horizontal variations in air pressure[7], then the pressure at the surface is constant within the area under consideration and equal to the atmospheric pressure. Thus, the surface is an isobar and we can set z_2 to be the level of the surface.

Let us consider two positions, site 1 and site 2, some distance apart, as illustrated in

7. This is a reasonable assumption if the horizontal length scale involved is small compared to the length scale of atmospheric pressure systems, such that the atmospheric pressure is approximately the same over the entire area being studied.

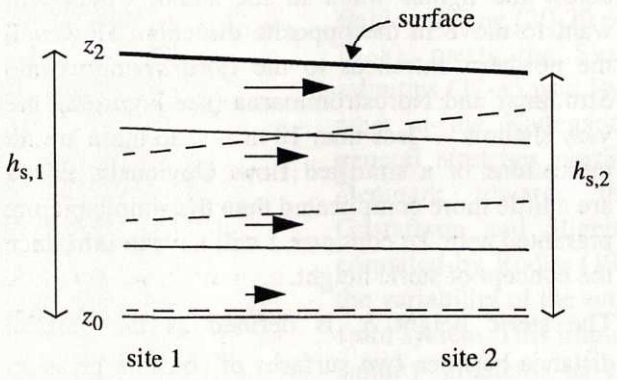

Figure 3. This schematic illustrates the steric height difference between two sites with different stratification. The dashed lines are isopycnals, showing how there is heavier water nearer the surface at site 2, and the solid lines are isobars. At the level of no motion the pressure gradients due to the higher surface level at site 1 exactly cancels that due to the heavier water at site 2, and the isobars become horizontal. The large arrows indicate the resulting flow.

Figure 3. If there is no movement of water below some depth level z_0, then there can not exist any pressure gradient, or in other words pressure difference, between the two positions below z_0. This *level of no motion* is then an isobar. We can thus calculate the steric heights $h_{s,1}$ and $h_{s,2}$ at the two sites from equation (1) by integrating from the common depth z_0 to the surface. If the stratifications $\rho_1(z)$ and $\rho_2(z)$ at the two sites are different, then the steric height will be greater at the site with the less dense water, say site 1. Consequently, the sea level must slope downwards from site 1 to site 2 (see Figure 3). At the surface at site 2, the pressure will be equal to the atmospheric pressure. At *the same level* at site 1, pressure will equal the atmospheric pressure plus the weight of the extra column of water due to the sea level difference. Hence, near the surface the higher pressure at site 1 will force a surface flow of water towards site 2. Further down, the greater density at site 2 will compensate for this sea level difference such that the baroclinic (density dependent) and barotropic (sea level dependent) pressure effects cancel at the level of no motion[8]. In summary, we

8. To be exact, in a barotropic flow isobars are parallel to isopycnals (surfaces of constant density) and thus the pressure forcing will be the same for all depths. In baroclinic flows isobars and isopycnals are not parallel, and density differences will produce depth-dependent pressure gradients.

can calculate the steric height difference $\Delta h_s = h_{s,1} - h_{s,2}$ from the density stratification at the two sites assuming that we know the level of no motion, and this in turn yields the surface pressure gradient forcing the barotropic component of the flow.

Channel flow

Before coming back to the fjord system, I will briefly describe how to calculate the flow in a channel subjected to only barotropic forcing due to a sea level difference, as described by Stigebrandt (1980). Consider a short channel, in which the flow is quasi-stationary (meaning very slowly changing, such that variations in time may be neglected) and friction is insignificant. The fundamental equation of motion will then reduce to a balance between pressure gradient and inertial forces, that is

$$\vec{v}\nabla\vec{v} = -\frac{1}{\rho}\nabla p$$

where $\vec{v}$ is the velocity vector, p the pressure field and ρ the density. If we integrate this equation from far upstream the channel, where because of the large width the magnitude of $\vec{v}$ is very small, to the channel, where the flow speed is, say u, we get the Bernoulli equation

$$\eta_1 = \frac{u^2}{2g}, \qquad (2)$$

in which g is the acceleration of gravity. This means that we require a sea level drop of η_1 meters to accelerate the water from rest to the speed u in the channel. If we now consider bottom friction, where the friction force depends on the friction coefficient C_D, the square of the flow speed and the bottom area, we can calculate the sea level drop η_2 necessary to balance the friction force according to

$$\rho\eta_2 gA = \rho C_D u^2 BL. \qquad (3)$$

Here, A is the cross-sectional area of the channel, B is the length of the wet perimeter and L is the length

of the channel. Adding the two effects described by equations (2) and (3), we find that

$$\eta = C_M \frac{u^2}{2g}, \qquad (4)$$

where η now is the total sea level drop between the ends of the channel and

$$C_M = \left(1 + 2C_D \frac{BL}{A}\right).$$

Thus, knowing η, the geometry of the channel and the friction parameter we can calculate the flow speed u (and hence the volume flux), assuming that the flow is barotropic.

Hypothesis

Now let us apply the concept of steric height to the Orust-Tjörn fjord system. Because of the runoff to the Baltic Sea[9], on average we should expect a higher sea level in the Baltic Sea than in the North Sea. This sea level difference drives the excess surface water out of the Baltic Sea, through the Danish straits and the Kattegat and on through the Skagerrak along the coasts of Sweden and Norway. To counter friction and other losses of momentum, a continuously sloping sea level is required. Hence, we would expect, on average, higher sea levels along the southern parts of the Swedish west coast and lower further north. There are indications that such a sea level difference exists. Both Gustafsson and Stigebrandt (1996) and Ekman (1994) found significant long-term sea level differences along the Swedish coast in the Skagerrak, using different techniques. It is this sea level slope that we propose is the driving force behind the net counterclockwise flow through the Orust-Tjörn fjord system. Unfortunately, horizontal sea level gradients and their variations are notoriously difficult to measure, in particular because of the problem of determining a common reference level. This brings us back to the concept of steric height.

9. The yearly average freshwater input to the Baltic Sea is approximately 15000 $m^3 s^{-1}$.

As discussed earlier, if at some depth there is to be no horizontal pressure gradient (level of no motion), which I will soon show is a reasonable supposition, then the pressure difference due to the sea level slope must be compensated for by baroclinic pressure gradients. In other words, the mean density of the water column must increase towards the north, and the density stratification will continuously adjust to compensate for variations in the sea level slope. The adjustment process will involve the advection[10] of water by density-driven flows. Using the concept of steric height we can then calculate the sea level difference between the ends of the fjord system from the difference in stratification.

It is of course not always obvious where the level of no motion is, or even if there is such a thing. In our case, we had no choice as most of the data on the stratification outside the entrances to the fjord system did not go deeper tha n 20m. However, in this area of strong stratification the halocline[11] is usually found above this level[12]. Since tilting of the halocline will more or less eliminate pressure gradients below it, flow velocities will only rarely be significant below 20 m. Thus, the error we make in setting the level of no motion to a depth of only 20 m is not very serious. In fact, doing the calculations for the instances when deeper measurements were available yielded no large change in the computed steric heights, as discussed in Paper I.

To summarize, the hypothesis is that an unknown sea level gradient along the coast drives a counterclockwise flow in the upper layers of the

---

10. The bodily transfer of a property by a flow, in contrast to diffusion where a property may be transferred without a net volume flux.

11. The intermediary, often thin, layer between two water masses of different salinities.

12. An analysis I performed for entirely different reasons at SMHI, using long-term data from Vinga, yielded an average halocline depth of 15 m.

fjord system, and this gradient will in turn be related to a gradient in the density stratification in the opposite direction, which we can measure. The testing of this hypothesis is the main theme of Paper I.

The straits of Malö Strömmar

As will be described in the summary of Pape rI, my colleagues and I not only showed that the steric height difference could be the cause of a net flow through the Orust-Tjörn fjord system, but also measured such a net flow, both in Nötesund and in Malö Strömmar. In the former case, we deployed an acoustic current meter called an ADCP (Acoustic Doppler Current Profiler) on the bottom of Nötesund, and analyzed the current measured by this instrument. In Malö Strömmar, however, we used a quite different method for determining the flow through the straits.

To begin, one tide gauge[13] was deployed on each side of Malö Strömmar, at Ellös and at Morlanda, as well as in the intermediary basin. The idea was that if we could determine the sea level difference we should be able to calculate the flow, since the former drives the latter. However, there are two problems. First, we must find a common reference level for the tide gauges, since it is impossible to deploy them at exactly the same level. Secondly, we must take into account other processes affecting the flow, such as friction. Therefore, recording current meters (RCMs) were deployed for short periods in Björnsund, the narrowest of the two channels in Malö Strömmar. You might ask why we did not simply use the RCMs to determine the net flow? The reason is that they are susceptible to biofouling, such as seaweed getting stuck in the rotor, as well as being run over by boats. We needed long records, several weeks at the least, and few of the RCMs worked for more than a week at a time.

13. An instrument which measures the pressure, from which the height of the column of water above it — and hence the sea level variations — can be calculated.

The tide gauges were leveled by assuming that the sea level difference across Malö Strömmar should be zero at slack water, or in other words, no current, no sea level difference (compare Figure 3). I then used a least-squares fitting procedure to determine the constant C_M that would produce the best agreement between measured and calculated current. Since the friction coefficient is usually of the order 10^{-3}, then knowing the approximate length, width and depth of Malö Strömmar we can make a crude estimate of the value of C. This yields $C_M \approx 2$. My fitting yielded values between 2.3 and 2.9. In Paper 1 we have used the value 2.7. It should be mentioned that the good agreement between the measurements and the fitted curve as well as the reasonable value for C_M supports the validity of equation (4).

To take a closer look at how the tidal fluctuations affect the barotropic flow in the narrow channels of Malö Strömmar[14], I devised a numerical one-dimensional model which included a more detailed topography, much in the fashion of Robinson et al. (1983). First, I divided Malö Strömmar into 24 irregular compartments, or boxes, and from a chart estimated each box's average depth H, the widths of the cross-sections delimiting each box B, and the average width of each box $\overline{B}$. Then the equations to be solved are the one-dimensional equations of motion and of continuity in a rectangular channel of variable width and depth;

$$\frac{\partial u}{\partial t} + u\frac{\partial u}{\partial x} = -g\frac{\partial h}{\partial x} - C_D\frac{u|u|P}{\overline{B}(H+h)} \qquad (5)$$

and

$$B\frac{\partial h}{\partial t} + \frac{\partial}{\partial x}\{\overline{B}u(H+h)\} = 0. \qquad (6)$$

14. See also the appendix in Paper I, which addresses the problem of tidal choking.

Here, $u(x)$ is the average current for a cross-section at position x in the along-channel direction, $h(x)$ is sea level measured from some reference level, $P = \bar{B} + 2(H + h)$ is the wet perimeter and t is time. Equation (5) describes how the flow velocity accelerates or decelerates, both in time and in space, due to the different forces acting on the flow. The forces are found on the right-hand side; a pressure gradient force caused by a sloping sea level (first term) and bottom friction (second term). Equation (6) makes sure that no water is created or lost in the boxes, so if there is more water coming into a box than going out, then the sea level h must go up in that box. The two equations were applied to the chain of boxes by calculating u at the boundaries between the boxes and h in the centre of the boxes, a so-called staggered grid arrangement. For the technically interested, the discretization was performed using the angular derivative method (see, e.g., Kowalik and Murty 1993, p. 51-52) and a semi-implicit bottom friction term.

The ends of the computational grid were located outside the ends of Malö Strömmar, such that the model would calculate the sea level drop due to acceleration into the straits. However, at the downstream end the flow is likely to form a jet, unless the flow speed is small. This means that the kinetic energy of the flow will be lost through intensive turbulence, instead of reverting back to potential energy in the form of a rise in the sea level. To model this, I assumed that if the magnitude of the flow speed was greater than some critical value, say u_c, the balance in equation (5) would be between the deceleration term and the friction term, that is

$$u\frac{\partial u}{\partial x} \approx -C_D^{jet}\frac{u|u|}{H}$$

for $|u| > u_c$. If the scales for u, $\partial/\partial x$ and H are U, $1/L$ and H', respectively, then

$$\frac{U^2}{L} \sim C_D^{jet} \frac{U^2}{H'} , \qquad (7)$$

which implies that

$$C_D^{jet} \sim \frac{H'}{L} . \qquad (8)$$

Hence, I model the jet downstream of an abrupt widening by setting

$$C_D = C_D^{jet} = K_{jet} \frac{H}{\Delta x} \qquad (9)$$

in the relevant box, where Δx is the length of the box. Comparisons between computed and measured u in Björnsund, using a least-squares estimate, showed that $u_c = 0.2$ m s^{-1}, $C_D = 0.013$ and $K_{jet} = 6$ were suitable values.

In Figure 4 (overleaf) I have plotted the observed along-channel current in Björnsund over a 48-hour period in November 1995[15]. Also shown is the current calculated from the observed sea level difference. The curve labeled "stationary" was computed using the simple, quasi-stationary model given by equation (4), with $C_M = 2.35$, whereas the numerical solution of equations (5) and (6) is termed the "advanced" model.

It is obvious that both models do a good job of replicating the observed current. However, if we take a look at the details, the advanced model follows the observed time series more closely, particularly when the current changes direction. The stationary model does a somewhat better job of simulating the current during outflow (negative values), when the advanced model slightly underestimates the current speed. Even so, the advanced model yields a mean current over the entire period of -0.4 cm s^{-1} whereas the stationary model yields 2.9 cm s^{-1}, compared to -16.4 cm s^{-1} for the

15. The measurement record is actually two weeks long, but the 48-hour period shown is typical for the entire record.

observed current. Thus, both models overestimate the mean current velocity, though the advanced model at least yields a value smaller than zero. A consequence of these results is that the flow resistance of Malö Strömmar is not symmetrical with respect to flow direction.

The mismatch between observations and the stationary model during slack water, is most likely a consequence of neglecting the time derivative[16] $\partial u/\partial t$ in equation (5). When the current speed is close to zero, both the term $u\partial u/\partial x$ and the friction term will also be nearly zero. Hence the pressure term $g\partial h/\partial x$, though relatively small as well, can only be balanced by the time derivative. Neglecting the latter also implies that a change in the sea level difference immediately produces a corresponding change in current. In reality, it will take some time before the current has adjusted to the change in the forcing. A cross-correlation between the sea level difference and the mean current in the strait yields a maximum correlation for a lag of approximately 15min. Thus, there is a time lag of about 15 min between a change in the sea level difference and the response of the flow.

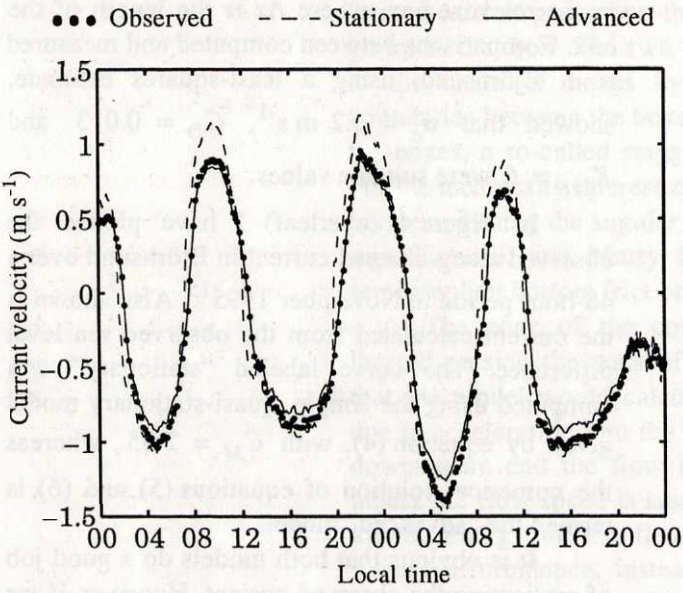

Figure 4. Observed and modeled along-channel current velocities in Björnsund 19-20 November 1995.

16.The time derivative term describes the local acceleration of a small water parcel.

2.3 Deep water renewal and entrainment

In the previous section the circulation above sill level was discussed. We will now turn to the water in the deep basin below sill level. As mentioned in the beginning of the present chapter, fjords go through an irregular cycle of stagnation and renewal. The focus of the present section will be on renewals, and in the next chapter I will continue by discussing stagnation. The common view of this stagnation/renewal chain of events is as follows (see, e.g., Gade and Edwards 1980).

The common view

After a renewal event, the deep water inside a fjord is isolated from outside by the sill and from the surface waters by a strong pycnocline[17]. If this deep water retained its initial density, a new renewal would require even denser water to enter from outside, which would have to be followed by an even denser inflow, and so on. Instead, weak turbulent diffusion slowly mixes the deep water with less dense surface water. Eventually the deep water density has decreased sufficiently for a new inflow to take place and the cycle starts over. How this weak turbulent diffusion can be included in a numerical model of a fjord is the subject of Paper III, and will be discussed in Chapter 3.

The forgotten entrainment

However, in the description above I have neglected the details of the actual renewal event. A common simplification when calculating the effects and size of a renewal is to assume that the dense, juvenile water that enters the fjord flows down the bottom slope and interleaves at a depth of equal density, without really altering its properties (e.g., Allen and Simpson 1998). In fact, much can happen before the juvenile water has founds its place in the deep basin. Particularly, the plume of juvenile water most

17. This is a sharp vertical gradient in density, caused by a jump in salinity and/or temperature. For the Swedish reader, this is what we commonly call "språngskikt" (see also halocline).

likely undergoes substantial mixing with the less dense resident water on its way to the deep basin. Though it may of course be justified to neglect this mixing in some cases, in Paper II my co-authors and I show that the entrainment flow, that is the flux of resident water into the juvenile water due to mixing, may be several times larger than the inflow of juvenile water itself.

So far I have neglected to mention mixing between inflowing juvenile and outflowing resident water on the sill, before the formation of a bottom plume (see, e.g., Gillibrand et al. 1995). This will of course affect the initial properties of the plume and increase the total mixing between juvenile and resident water. The degree of sill mixing depends on the sill flow as well as the length and width of the sill. I will not discuss this process any further here, and will only mention that it is briefly discussed in Paper II.

Consequences

Extensive mixing between juvenile and resident water has several important consequences. Most are obvious and were recognized early on, but in my opinion they are not always clearly stated and sometimes, intentionally or not, left out completely. Unfortunately, this is to some degree the case for two of the most comprehensive reviews on fjord circulation and dynamics (Gade and Edwards 1980; Farmer and Freeland 1983), which may give rise to some confusion. Below I will attempt to summarize some effects of mixing during inflows which are less often mentioned.

First, one implication is that even though the density can be seen to have increased at all levels in the deep basin after an inflow, the basin water need not have been completely renewed. Old resident water may still remain in the basin waters, mixed together with the juvenile water.

This leads to the second effect, namely that vigorous entrainment of less dense resident water into the inflowing juvenile water will delay the complete flushing of all the resident water, since some of the resident water — albeit smaller and smaller fractions as time passes — will be

continuously recirculated. Hence, a renewal may only be partial even if the total inflow of juvenile water exceeds the total volume of the fjord basin.

Finally, if a renewal does not persist long enough for all the resident water to be flushed out of the fjord, implying a partial renewal in the sense described in the previous paragraph, the post-renewal basin water will be less dense than the juvenile water entering from outside. The fjord may then be primed for a new renewal immediately. The somewhat controversial conclusion is that reduction of the deep basin densities by interior diffusion is no longer as significant for the occurrence of a subsequent renewal. Instead, exterior processes will be the dominating factor determining the occurrence of the next renewal. This is illustrated in Figure 5. Diffusion by itself is unable to lower the basin water density sufficiently for there to be an inflow in the middle of the time period, as shown in (A). However, if there is mixing between juvenile and resident water during the first renewal, the slow density reduction caused by diffusion is sufficient to yield a second inflow at the second peak in the exterior density curve (B). Over long time scales, that is, over several renewals, interior deep basin mixing is of course necessary, since mixing during a renewal cannot decrease the density of the inflowing water to that of the resident water. If there

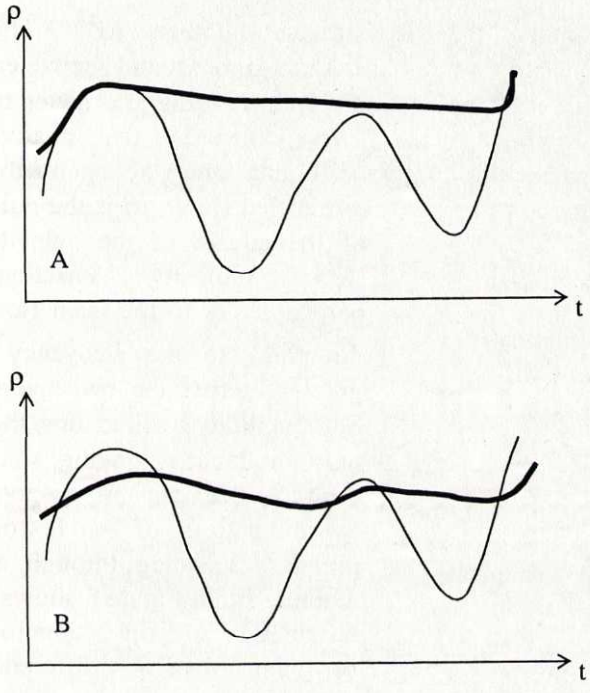

Figure 5. This schematic shows the possible effect of entrainment (not to scale). The curves are the density variations with time ρ(t); light lines represent variations outside the fjord and heavy lines represent variations in the deep water inside the fjord. In (A) there is no entrainment and in (B) entrainment is included.

was no interior mixing during stagnation, but only mixing during inflows, the deep water density would increase, though slowly, with each new inflow until no more renewals could occur.

To conclude, the points raised above emphasize the necessity of a quantitatively accurate parameterization of the mixing/entrainment process.

The Richardson number

When discussing entrainment the state of a flow is often described by a single important parameter, namely the Richardson number Ri[18]. The Richardson number is a non-dimensional parameter, that is, it has no unit such as kilogram, meter or likewise. Instead, Ri expresses the relative magnitudes of two different forces acting on the flow. In two-layered stratified flows, Ri is the ratio of the square of the velocity shear (velocity variations perpendicular to the main flow direction) to the buoyancy[19] gradient across the two layers. For simplicity I will assume that only one layer is moving, since such a scenario is a good approximation of a bottom plume descending through an ambient fluid. Figure 6 shows a schematic of the situation. Gravity acting on the density difference $\Delta\rho = \rho_2 - \rho_1$ stabilizes the flow and hence decreases mixing between the two layers. A simple explanation is that the lighter layer wants to stay on

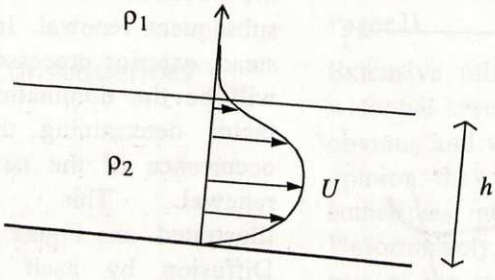

Figure 6. A schematic of a bottom plume flowing down an inclined slope.

18. Also termed the overall, bulk or layer Richardson number (Turner 1973; Fernando 1991). There are also gradient and flux Richardson numbers, which will be discussed later.

19. The term buoyancy refers to the upwards or downwards force felt by small water parcel because its density differs from the surrounding density. It equals the density difference times the acceleration of gravity. Henceforth I will mix the terms density gradient (or difference), buoyancy gradient (or difference) and stratification, as they are interlinked and all describe the degree of stratification.

top and the heavier layer below. The velocity shear, on the other hand, acts to destabilize the flow and hence to increase mixing. In this case one could say that a velocity shear will tend to create turbulent vortices and whirls, almost for the same reason that you would likely fall on your face if the upper part of your body moved faster than your feet. The shear $\partial u/\partial x$ is "approximated", or scaled, as U/h where U is the mean velocity of the moving layer and h is the thickness of the layer.

The Richardson number is in this case[20] defined as

$$Ri = \frac{g'h}{U^2}, \tag{10}$$

where

$$g' = g\frac{\Delta\rho}{\rho_2}$$

is called the reduced gravity. If Ri is large, the stabilizing buoyancy force dominates and we may expect little mixing. If Ri is small, then the shear is large compared to the buoyancy force and the flow will be strongly turbulent yielding large mixing between the two water masses.

Taking the square root of Ri yields

$$\frac{\sqrt{g'h}}{U},$$

which is the ratio of the speed of a long internal wave[21] on the interface between the two layers, and the flow speed. Hence, if $Ri < 1$ then a long interfacial internal wave cannot propagate upstream, because its speed is smaller than the flow speed. This is called a *supercritical* flow with respect to the phase speed of a long internal wave.

---

20. There exists different formulations depending on the flow configuration and type of forcing.

21. This can be compared to the speed of a long wave on the surface which is the square root of gD, where D is the depth of the water. A long wave has a wave length greater than D.

The opposite is called a *subcritical* flow ($Ri > 1$). The *critical Richardson number* is thus $Ri_c = 1$.

The entrainment process

Before discussing different formulae for calculating entrainment, I will present a brief and very simplified description of the processes that produce mixing at a density interface. One reason is that this will serve as a useful background to the topic of the following chapter, turbulence modeling. Another is to show the complexity of interfacial mixing. My presentation will primarily be based on the article by Christodoulou (1986) referred to earlier, the review by Fernando (1991) and the recent work of Sullivan and List (1994).

Mixing across gravitationally stable density interfaces is an important process, both when studying geophysical phenomena, such as the development of the upper-ocean mixed layer (important in climate modeling), and in engineering applications, for example, the spreading of hot water discharges from power plants. However, as stated by Fernando (1991), despite almost a century of research we still lack universal laws quantifying this fundamental process.

To describe the regimes in which different physical mechanisms dominate the mixing process I will use an unspecified Richardson number *Ri*. I will therefore not present any values but only use terms such as "small", "intermediary" and "large" to give some general idea of the type of flow.

Consider two homogeneous layers separated by a narrow interface in which the density changes from that of one layer to that of the other (see Figure 6). Again let us assume, for simplicity, that only one layer is moving and turbulent, whereas the other is at rest. This implies that there is a sheared boundary layer[22] incorporating the density interface. For small values of *Ri* the flow is everywhere turbulent, even in the pycnocline

22. A boundary layer is a region near a boundary where flow properties change from that on one side of the boundary to that on the other.

separating the two layers. Small-scale turbulence penetrates the density interface and lifts fluid from the non-turbulent layer into the turbulent layer, where it is rapidly mixed.

For intermediary values of *Ri*, where the density interface itself is no longer turbulent, another process takes over. Large-scale turbulent eddies[23], or whirls, in the turbulent layer scour fluid of intermediate density from the edge of the interface. If this was the only active process, the interface would become sharper and sharper as time progressed, further inhibiting mixing between the two layers. Hence we require some process which creates mixing at the edge of the interface, thickening it and producing water of intermediary densities which may be scoured off by the turbulent eddies. For low intermediary values of *Ri* the relevant process may be Kelvin-Helmholtz instabilities. These are formed at sheared density interfaces under certain conditions in which the destabilizing effect of shear overcomes the stabilizing effect of the density gradient. Their appearance is like narrow waves that curl up without breaking. Kelvin-Helmholtz instabilities may evolve into turbulent billows, producing localized mixing which then spreads as an intrusion along the edge of the interface. This mixed water can then be scoured off and incorporated into the turbulent layer.

For higher intermediary *Ri*-values, Kelvin-Helmholtz instabilities do not arise. Instead interfacial waves are formed, presumably generated by random pressure fluctuations induced by turbulent eddies, which eventually break due to the destabilizing effect of the mean shear. However, when these waves break much less mixing appears to occur than in the case of Kelvin-Helmholtz instabilities.

---

23. With the term "large-scale" I refer to the most energetic eddies, in general those generated by the mean flow (see chapter 3).

The processes described so far, primarily based on the observations of Sullivan and List (1994), are similar to those proposed by Bo Pedersen (1980), also cited by Christodoulou (1986) and Fernando (1991). Bo Pedersen distinguished between two fundamental types of entrainment. For low *Ri* — supercritical conditions — vortices are formed on the interface. These coalesce to form larger eddies which eventually are removed from the turbulent interface ("vortex entrainment"). When *Ri* is high, wave-like undulations are instead formed on the interface. These occasionally form cusps which may be detached and incorporated into the turbulent layer by large-scale eddies ("cusp entrainment").

As *Ri* becomes even larger, molecular diffusion becomes important. When *Ri* is sufficiently large this is the only process which can thicken the interface.

Entrainment formulae

In Paper II we discuss and test some of the formulae that have been proposed for calculating the entrainment[24] into a bottom plume. The most commonly cited work on entrainment in dense gravity currents is probably the laboratory study of Ellison and Turner (1959). Their results were later summarized by Turner (1986), in a formula that has become popular among oceanographers and has been applied to, for example, bottom plumes related to marginal sea overflows (e.g., Price and Baringer 1994; Borenäs and Wåhlin 2000). Turner's formula is an empirical function of the Richardson number *Ri* and the slope, and yields zero entrainment for subcritical flow (see Paper II).

In his detailed monograph on two-layer stratified flows, Bo Pedersen (1980) presents an alternative formula which depends on a constant *flux* Richardson number[25], the slope, the friction

24. The concept of entrainment is obviously a simplification of the complicated processes that cause mixing across the interface separating two flows. In the words of Turner (1986) "the entrainment assumption [relates] the inflowing velocity to the local mean velocity of a turbulent flow".

coefficient, the velocity profile, the interfacial velocity and the degree of turbulence. Bo Pedersen then proceeds to simplify this rather complicated formula to an expression depending on the friction coefficient and the slope, setting the remaining variables to different constant values depending on whether the plume is super- or subcritical. The state of the flow is in turn determined by the slope. Further simplifications yields that the entrainment is directly proportional to the slope only. This simple formula, by the way, is identical to that determined by Stigebrandt (1987) for the subcritical dense inflows to the Baltic Sea. Hence, this formula works well for flows along gentle slopes.

Finally, based on a compilation of available entrainment experiments and theoretical considerations, Christodoulou (1986) proposed a combination of different functions of *Ri*, where the choice of function depends on the dominating type of entrainment mechanism and is indicated by the value of *Ri*.

Effects of entrainment

In Paper II the three different formulae introduced above are compared. The most interesting result of this comparison is that the formula by Turner (1986) yields the poorest agreement with observations. Since entrainment is zero for subcritical flow, Turner's formula yields no entrainment in the early parts of the plume, where the bottom slope is gentle. The other two formulae produce entrainment along the entire path of the plume, although it is small where the slope is gentle. Even so, because of the larger salinity difference, the weak entrainment in the upper sections of the plume have a profound effect on the final properties of the plume. Although the total entrainment for a plume that reaches all the way to the bottom is larger if Turner's formula is used, the salinity is higher because almost all of the entrainment takes place on the steep slope near the

25.This Richardson number is the ratio of production of turbulent kinetic energy by the mean shear to the destruction by the stratification; see chapter 3.

bottom, where the salinity difference small. I should mention that the measurements of Ellison and Turner (1959), upon which Turner's formula is based, were limited to steep slopes greater than 12°. Such steep slopes are probably rare in nature.

In Paper II we have chosen the formula by Bo Pedersen (1980) as the standard configuration. However, despite being quite different both in its functional form and calculated entrainment, the formula of Christodoulou (1986) yielded very similar results. Since Bo Pedersen's formula is primarily dependent on the slope, it is probably not very suitable for rotational flows, where a balance between the Coriolis force[26] and the buoyancy force will tend to make the bottom current follow the isobaths (depth contours) rather than descend straight down the slope. Personally, of the three formulae presented here, I would therefore recommend the formula of Christodoulou. This formula also shows very good agreement with measured or estimated entrainment over the entire span of investigated Richardson numbers.

The process of entrainment has interesting consequences for the behavior of a bottom plume, some of which are not immediately intuitive. I will therefore summarize some results from the modeling of the 1974 renewal event in Byfjorden which are only very briefly mentioned, or not pointed out at all, in Paper II. To begin, the average ratio of entrainment flow to initial plume flow

$$R_e = \frac{Q_e}{Q_d^0}$$

was found to be about 2.5. This means that the final plume volume flux before interleaving was on average 3.5 times the initial flux at sill depth. For comparison, the Christodoulou formula yields on average a somewhat larger R_e, about 2.8.

The interleaving depth was inversely correlated with the entrainment ratio, such that large

26. An effect due to the rotation of the earth.

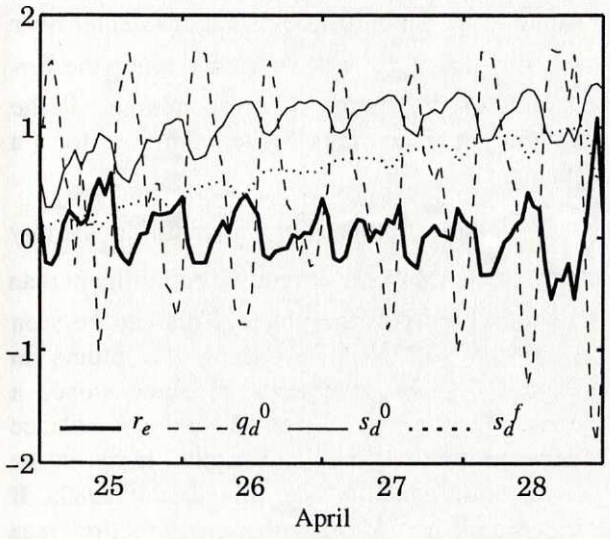

Figure 7. Modeled time series of the normalized entrainment ratio r_e, initial plume flux q_d^0, and initial and final plume salinities s_d^0 and s_d^f for four days in April 1974.

entrainment produced interleaving at a shallower depth. This is of course what we would expect, as increased entrainment implies more mixing with resident water and hence a stronger reduction in the plume's density. On a few occasions during the early part of the renewal period the entrainment ratio reached as high as 10, or in other words, the entrainment of resident water into the plume was 10 times the initial flow of juvenile water over the inner edge of the sill.

In Figure 7 I have plotted an example of the temporal variations of R_e, Q_d^0 and the initial and final plume salinities S_d^0 and S_d^f, based on the results of the standard configuration. To make comparison easier I have normalized each variable by deducting the mean value and dividing by the standard deviation. Thus, for variable X the normalized value, signified by a small letter, is given by

$$x = \frac{X - \bar{X}}{\mathrm{std}(X)}.$$

All normalized values will then vary around zero. The following features may be discerned.

1. The initial plume flux q_d^0 is inversely correlated with the initial plume salinity s_d^0. This is a consequence of the sill flow parameterization, or in other words how the inflow through the mouth

takes place before the plume is formed. A small flow implies that only the really dense, high-saline water from outside manages to enter over the sill. Hence s_d^0 will be higher, since the formation of the plume involves mixing all the entering juvenile water dense enough to form a plume.

2. A large plume (large q_d^0) of lower initial salinity s_d^0 experiences a lower relative entrainment than a small, highly saline plume. This can be seen from the equations describing the plume in Paper II if we assume a constant slope, a constant entrainment rate and a local balance between the buoyancy and friction terms in the momentum equation (see Stigebrandt 1987). If the plume has a triangular cross-section (see Paper II) then the simplified momentum equation and the continuity equation together yield that the "specific dilution", that is, the ration between the local entrainment flux and the plume's volume flux[27], is proportional to $Q_d^{-2/5}$, where Q_d is the plume flux. This shows that if you increase the plume flux, the relative entrainment decreases. However, if the entrainment rate is not only a function of the slope, as in Bo Pedersen's formula, but also of the flow properties (described by Ri), as in the formulae of Christodoulou and Turner, then the relationship is not as straightforward. Again using a triangular cross-section, it can be shown that

$$Ri \propto \frac{g' h^5}{Q_d^2}.$$

27. This is almost the same as R_e in our case.

Hence, a larger volume flux will decrease *Ri*, but if the plume is also bigger in size then *Ri* will increase. Since larger plumes tend to be associated with lower salinities in the model, g' will also act to increase *Ri* for large plumes.

3. The final plume salinity s_d^f is higher when the initial plume flux is larger, but negatively correlated with r_e and s_d^0. This means that large, less saline plumes will yield higher final salinities. This is of course because the relative mixing with the resident water is smaller, and hence a large plume will retain its properties more efficiently. However, note that the variations in the final plume salinity are very small in comparison to the variations in the initial conditions and total entrainment. The most likely reason is that the mixing is at all times large compared to the difference in properties between the inflowing and resident water. For example, if you add 2 m^3 of water with salinity 28 to 1 m^3 of water with salinity 30, the resulting salinity will be 28.7. Instead adding 5 m^3 of the low salinity water will yield a mixture of salinity 28.3. The difference is small compared to the salinities involved, but may of course be significant in the long run.

I will conclude this section by stating that it now appears as though we can model fjord renewals with fair accuracy, including mixing due to entrainment. However, a truly universal parameterization of mixing across a density interface is yet to be found. This brings us to the topic of the next chapter, namely turbulent mixing.

3 Turbulent mixing

This chapter deals with certain details of turbulent mixing and how these can be quantitatively modeled in geophysical[1] flow systems. Turbulence remains one of the most important unsolved problems in physics. In the millennium issue of Scientific American (December 1999) physicist Steven Weinberg, in his article "A unified physics by 2050?", writes as follows:

> "The discovery of a unified theory that describes nature at all energies [...] will not be the end of physics. It probably won't even help with some of the outstanding problems of today's physics, such as understanding turbulence and high-temperature superconductivity."

Now, high-temperature superconductivity may seem an academic, esoteric subject, though it is of course of great interest to the power industry and the information technology business. Turbulence, on the other hand, is all around us all the time. Turbulence is responsible for mixing the sugar in your tea, or the petrol and air in your car engine. If you put a teaspoon of sugar in your cup and let molecular diffusion by itself perform the mixing, your tea will be cold long before you can taste any sweetness. Turbulence is the major complication when analyzing any fluid flow, be it the flow of water in your pipes at home, or the oceanic and atmospheric flows determining the weather and climate. Of course, there are numerous applications highly relevant to the industry as well (see, e.g., Revstedt 1999).

What is turbulence?

Turbulence is usually described as chaotic, energetic, whirling motions in a fluid flow.

1. I use the term geophysical as meaning physical processes in nature on the scale of rivers, lakes and up to oceans or the atmosphere.

Furthermore, turbulence is a property of the flow, not of the fluid. Hence, there will be very little turbulence in a pond on a calm day, whereas a fast-flowing stream will be very turbulent. The same applies to your tea. It will be non-turbulent unless you stir it. This is in contrast to, for example, molecular diffusion, which is the same for all flows of a particular fluid. Molecular diffusion acts to homogenize the properties of a fluid, but is only efficient over very small distances. The effect of turbulence is to stir the fluid by advecting and straining fluid parcels, and hence to enhance the irreversible mixing taking place at the small scales where molecular processes become important.

Turbulent motions can take place on varying spatial and temporal scales, that is they can affect the fluid over different distances and for different lengths of time. However, the largest motions will be limited by the length scale, or size, of the flow, and the smallest by the dissipating effect of molecular diffusion. More about this later.

My simplified, intuitive picture of turbulence includes a variety of whirls, or turbulent eddies, of different sizes l and intensity of motion q (see, e.g., Tennekes and Lumley 1972). This is illustrated in Figure 8. Large, energetic eddies are formed as a result of instabilities in the mean, or large-scale, flow[2]. In the previous chapter I described entrainment across a density interface. If we for a moment forget the density difference, and just imagine two flows of different velocities, then the velocity shear between the two will create "overturning" motions, or eddies. The shear destabilizes the fluid and produces turbulence, as described in section 2.3.

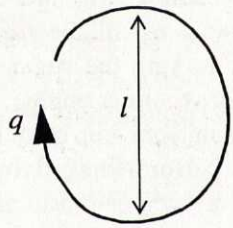

Figure 8. An illustration of a turbulent eddy.

These large eddies then interact with each other and the mean flow, producing smaller eddies. This *cascade* of turbulence, from larger to smaller eddies, eventually produces eddies small enough for molecular *viscosity*[3] to become important.

2. The mean flow will be more rigorously defined in the following section.

Molecular processes smear out the remaining velocity differences between the eddies and the mean flow, destroying the eddies. This process is called *viscous dissipation*, and converts the *turbulent kinetic energy* (TKE) of the turbulent motions to heat. Thus the molecular fluid properties determine the smallest scales at which turbulence can exist. As briefly mentioned earlier, it is on these small scales, on the order of a few centimeters or less, that the actual mixing takes place, that is the transport of different fluid properties across gradients in these properties. Through its stirring effect, the turbulence acts to create and maintain such gradients at these small scales and hence to greatly enhance mixing (Toole 1998).

Before discussing what I have done, I will attempt to summarize the approach to turbulence that has been dominating turbulence research and modeling during the last 30 years or so. This summary will primarily be based upon the review by Speziale (1991). I will only touch upon new developments, such as Large Eddy Simulations (LES) and Direct Numerical Simulations (DNS), as their applications to geophysical flows are still limited. Furthermore, I will not mention so-called mixed layer models — which in general do not attempt to calculate any turbulent quantities at all — even though these have been used in numerous applications with good results[4].

3.1 A brief summary of turbulence closure theory

The issue

All fluid flows can to a high degree of accuracy be described by the Navier-Stokes equations. Unfortunately, no one has as yet succeeded in finding a general solution to these equations for any

3. Viscous diffusion refers to momentum, whereas diffusion is the term used for such properties as salt, temperature, etc.
4. See, e.g., Large (1998) for a comprehensive review.

flow of some complexity[5]. With the rapid increase in computer capacity, attempts are being made to solve the complete Navier-Stokes equations numerically. Despite the speed of modern super-computers such calculations, for example the aforementioned DNS, are still restricted to geometries and flows much simpler than those found in nature.

Hence, we have to *model* the fundamental equations. Let me side-track here for a moment. When a scientist talks about modeling, he or she means the process of constructing simplified mathematical formulae that will allow him or her to calculate a solution, which hopefully to some degree describes the phenomena being investigated. I will allow myself to "borrow" an excellent quote by John von Neumann, cited in the thesis of a close friend.

> "The sciences do not try to explain, they hardly even try to interpret, they mainly make models. By a model is meant a mathematical construct which, with the addition of certain verbal interpretations, describes observed phenomena. The justification of such a mathematical construct is solely and precisely that it is expected to work."

However, the term modeling is also used to describe the act of simplifying complex mathematical expressions such that a solution may be calculated[6]. This is what turbulence modeling is all about.

Reynolds-stress modeling

The most widely tested approach to modeling turbulence is that of Reynolds-stress modeling. This rests on the assumption that there is a separation of scales between turbulent and "mean" motions, such that we can distinguish between the two. Consider

5. Apparently, such a solution is on the top-ten "most wanted list" of mathematicians today...
6. Note that modeling also often is used in the sense of actually performing the calculations, i.e., doing simulations.

the Navier-Stokes equation for an incompressible, viscous fluid in the absence of rotation:

$$\frac{\partial u_i}{\partial t} + u_j \frac{\partial u_i}{\partial x_j} = -\frac{1}{\rho}\frac{\partial p}{\partial x_i} - g + \nu \nabla^2 u_i \qquad (11)$$

Here, the indices describe the three directions, x, y and z (the Einstein summation convention is used for repeated indices), u is the velocity, p is pressure, ρ is density, g is the acceleration of gravity and ν is the kinematic molecular viscosity. In short, the first term on the left hand side in equation (11) is the local rate of change with time, and the second is the inertia term related to the change of velocity in space. On the right hand side we have the effect of pressure gradients, gravity and viscosity, the molecular diffusion of momentum (compare equation 5 in section 2.2). Similar *transport equations* may be set up for such properties as salt and heat.

Now we perform a Reynolds decomposition, in which we assume that we can separate between mean (overbar) and fluctuating, or turbulent, (primed) components, such that

$$u_i = \bar{u}_i + u'_i, \quad p = \bar{p} + p' \ .$$

In statistically steady turbulence, that is, when there are no trends in the flow with time, the mean of any flow property is simply given by the time average. For flows which are homogeneous in space, we can use a volume average, whereas for more complicated flows the mean is taken to be the ensemble mean, that is, the average over a large number of repeated observations. Now, if we insert the Reynolds decomposition into equation (11) and take the average we end up with the momentum equation for the mean flow;

$$\frac{\partial \bar{u}_i}{\partial t} + \bar{u}_j \frac{\partial \bar{u}_i}{\partial x_j} = -\frac{1}{\rho}\frac{\partial}{\partial x_i}\bar{p} - g + \nu \nabla^2 \bar{u}_i - \frac{\partial \tau_{ij}}{\partial x_j}, \qquad (12)$$

where

$$\tau_{ij} = \overline{u'_i u'_j} \qquad (13)$$

is the so-called Reynolds-stress tensor[7]. Equation (12) for the mean flow is identical to equation (11) for the total flow, except for the Reynolds-stress term. The Reynolds stresses are the forces acting on a small fluid parcel due to the fluctuating, or turbulent, velocities u_i'. When deriving equation (12) it is assumed that the mean of the fluctuating variables, as well as the mean of a fluctuating variable times a mean variable, are both zero.

Hence, if we want to determine the mean flow we have to solve equation (12), using conservation of volume[8]. Unfortunately this does not constitute a *closed* set of equations, as there are more unknowns than there are equations. What we lack is a way of determining the Reynolds stresses in terms of the mean flow variables. This is called the *turbulence closure problem.*

The eddy viscosity concept

A simple method for determining the turbulent fluxes[9] is to make the *eddy viscosity assumption.* This implies that the turbulent fluxes can be modeled as down-gradient diffusion, for example, diffusion of momentum from an area of high velocities to one of lower velocities. This idea is based on a supposed analogy with molecular diffusion of momentum, but with a much higher viscosity. Thus,

$$\tau_{ij} = -\nu_t\left(\frac{\partial \bar{u}_i}{\partial x_j}+\frac{\partial \bar{u}_j}{\partial x_i}\right) , \qquad (14)$$

where ν_t is the eddy viscosity. Hence, the larger the mean velocity shear the larger the turbulent fluxes of momentum. We are then left with the problem of

7. Products of turbulent quantities are called second-moment terms.
8. This implies that volume cannot be lost or created, since the fluid is incompressible and mass is preserved.
9. A stress is a flux of momentum. Turbulent fluxes of course also affect other properties, such as temperature, salinity, etc.

determining the eddy viscosity ν_t. This requires a further assumption. If the turbulence can be characterized by a *single* velocity and length scale, as in Figure 8, then from dimensional analysis $\nu_t \propto ql$ [10]. So, how do we determine the turbulent scales q and l?

Turbulent kinetic energy

If we take the original Navier-Stokes equation for momentum (11) and subtract the equation for the mean flow (12), we get an equation for the turbulent momentum fluctuations. Since kinetic energy per unit mass is the same as the velocity magnitude squared, we can multiply the fluctuating momentum equation by the fluctuating velocity u'_i and the result is an equation for the turbulent kinetic energy k. However, this equation requires further modeling of terms containing the fluctuating variables u' and p' (see, e.g., Svensson 1978), again utilizing the gradient transport hypothesis[11]. Finally, considering only a one-dimensional case, that is, only transports and variations in the vertical are retained[12], the result is (see, e.g., Rodi 1987)

$$\frac{\partial k}{\partial t} - \frac{\partial}{\partial z}\left(\nu_k \frac{\partial k}{\partial z}\right) = P + G - \varepsilon, \qquad (15)$$

where

$$P = \nu_t\left[\left(\frac{\partial \bar{u}}{\partial z}\right)^2 + \left(\frac{\partial \bar{v}}{\partial z}\right)^2\right]$$

is the production of TKE by the mean velocity shear,

$$G = \frac{g}{\rho_0}\nu_\rho \frac{\partial \bar{\rho}}{\partial z}$$

---

10. The dimension of ν_t is $m^2\,s^{-1}$.

11. As we did when we made the eddy viscosity assumption.

12. We hence assume that mixing in a water column is determined locally in the horizontal sense. This implies that horizontal transports must be much smaller than vertical transports. This is also called the boundary layer approximation.

is called the buoyancy production or destruction of TKE by the mean stratification[13], and ε is the viscous dissipation of TKE. The latter is always a loss, as described earlier. Note that the eddy viscosity/diffusivity need not be the same for momentum, density (ρ) and TKE (k) as indicated by the different subscripts on ν. However, the different *turbulent diffusivities* are also assumed to be proportional to ql (see Section 3.2).

Since $q \propto k^{1/2}$ we can calculate the eddy viscosity according to

$$\nu_t = c_\mu k^{1/2} l \,, \tag{16}$$

where c_μ is a non-dimensional constant or possibly a function of the stratification (see, e.g., Burchard et al. 1998). This will be discussed further in Sections 3.2 and 3.3. On the basis of dimensional analysis we can estimate the dissipation according to

$$\varepsilon = c_\varepsilon \frac{k^{3/2}}{l} \,, \tag{17}$$

where c_ε is a constant of proportionality. What now remains to be determined is l.

Alternative closures

One way of achieving turbulence closure is to find a suitable algebraic formula for the turbulent length scale l. This could be related to the depth, the stratification and/or the turbulent kinetic energy (e.g., Luyten et al. 1996; D'Alessio et al. 1998). We then end up with a one-equation k-l model. In paper IV such a model is presented and compared with the two-equation k-ε model. In the latter model it is the dissipation ε that is calculated instead of l, and the turbulent length scale is then determined from equation (17). The transport equation for ε can also be derived from the Navier-Stokes equation, but a great deal of modeling and simplifying assumptions are required. The result is

13. A stable stratification will decrease turbulence and an unstable stratification will increase it.

$$\frac{\partial \varepsilon}{\partial t} - \frac{\partial}{\partial z}\left(\nu_\varepsilon \frac{\partial \varepsilon}{\partial z}\right) = (c_{1\varepsilon} P + c_{3\varepsilon} G)\frac{\varepsilon}{k} - c_{2\varepsilon}\frac{\varepsilon^2}{k}, \quad (18)$$

where $c_{1\varepsilon}$, $c_{2\varepsilon}$ and $c_{3\varepsilon}$ are empirical constants.

An alternative two-equation model is that of Mellor and Yamada (1982), in which they use a transport equation for the combined variable kl instead of ε.

Further developments

Models based on the eddy viscosity concept have a number of drawbacks. For example, the turbulent transports are always in the down-gradient direction just as molecular diffusion, whereas both observations and LES simulations (see below) indicate that counter-gradient heat fluxes are important (Large et al. 1994). Furthermore, eddy viscosity models are local, in that the mixing is determined by the local values of the turbulent properties. In nature, large-scale non-local features such as convection[14] and Langmuir circulation[15] may have a substantial impact on the mixing. Attempts to extend turbulent kinetic energy models to include counter-gradient and non-local features have been made by, for example, D'Alessio et al. (1998). Finally, none of the models discussed so far include the effect of internal waves in and below the pycnocline. This is the subject of paper III, in which an attempt is made to include the internal wave energy (IWE) in fjords to correctly model the weak turbulent diffusion in the deep basin water.

Instead of using the eddy viscosity concept it is possible to achieve closure by solving the Reynolds-stress transport equation explicitly, after some modeling of the third-order terms. Such a second-order closure model[16] can account for non-local as well as rotational effects. However, such models are generally too computationally expensive for geophysical applications. Furthermore, the

14. The large-scale overturning of water that is unstably stratified, i.e. top-heavy.

15. These are coherent, counterrotating vortices formed near the surface as a result of wind stress, and can be seen as streaks of foam and debris in the direction of the wind.

Reynolds decomposition assumes that we can separate between turbulent and mean motions. As emphasized by Gargett and Holloway (1984) this is questionable when considering, for example, the overlap in the ranges of temporal and spatial scales between turbulent motions and the internal wave field.

An alternative model for oceanic vertical mixing that does not involve transport equations of turbulent quantities, is the K-Profile Parameterization (KPP) model of Large et al. (1994). This model is based on empirical[17] formulae for boundary layer mixing, and specifically addresses such non-local features as convection. However, though the KPP model has proven a successful and popular alternative to TKE models, it also relies on relatively crude representations of the mixing in the interior water masses, outside the boundary layers (see the following section).

A fairly recent method for calculating turbulence is to use Large Eddy Simulations (LES), briefly mentioned before. The basic idea is to solve the fundamental equations of fluid motion on a computational grid, or mesh of points in space and time, fine enough to resolve the large turbulent motions. We then only have to model the really small turbulent motions. As most of the turbulent transports are performed by the larger motions, and since we have fairly good theoretical descriptions of how turbulence behaves at the small scales, this is not a serious problem. This method appears to show some promise, but the computational requirements still render it mostly impractical for use in large-scale geophysical modeling. However, LES models

16. As mentioned earlier TKE models are also referred to as second-order closures, which may be somewhat confusing as they model the second-order turbulent fluxes using the eddy viscosity concept. Perhaps they should be termed "semi-second-order", as the TKE (and sometimes the dissipation) is the only higher-moment quantity for which a transport equation is solved.

17. In other words, based on experiments and observations.

are developing rapidly and it has actually been suggested that they should serve as a benchmark for testing other, simpler models of turbulent mixing (Large 1998).

3.2 Deep water turbulent mixing in fjords due to internal tides

This section deals with weak turbulent mixing in the deep basin waters of a stagnant fjord, and how this may be included in a TKE turbulence closure model based on the eddy viscosity/diffusivity concept. In this particular case I use the two-equation k-ε model, but the method is most likely applicable to all eddy viscosity models that solve prognostically for the TKE.

The issue

As described in Chapter 2, the circulation in the deep basin waters in sill fjords is severely restricted. Between short periods of renewal, there is no advective in- or outflows to the deep basin and only turbulent diffusion[18] has any appreciable effect on the deep water properties. These stagnation periods may last for many years, during which diffusive exchange with the less dense upper layers slowly homogenizes the deep water and decreases its density. In the long run, this process is necessary for future renewals to occur (see section 2.3). Also, turbulent diffusion will transport, for example, oxygen from the surface waters through the pycnocline and down to the often oxygen-starved bottom waters.

The detailed mechanics of deep water diffusion are still unclear. This is an important issue not only in fjord oceanography, but also when considering the general oceanic circulation. Like in fjords, interior mixing[19] is necessary to ventilate the

18. In this context turbulent diffusion is the same as weak turbulent mixing.

19. In contrast to boundary mixing, which occurs near the surface, bottom or lateral boundaries.

deep ocean basins (e.g., Munk and Wunsch 1998). Also, Gargett (1984) showed how the parameterization of interior vertical mixing is crucial to the large-scale circulation patterns in the oceans. The interior mixing is furthermore an important factor when modeling the deepening of the near-surface oceanic mixed layer, where, for example, TKE models have a tendency to underestimate the mixing (e.g., Martin 1985).

What causes interior mixing?

In the deep basin waters of fjords, as well as in the abyssal ocean, the mean velocity and velocity shear fields are very weak. This is because the pycnocline at the bottom of the surface mixed layer effectively hinders the vertical transport of momentum (and other properties) from the surface to the interior. In essence, the pycnocline may be seen as a "slippery" layer insulating the interior from the boundaries, since the sharp density gradient stabilizes the flow and suppresses turbulence (see Section 2.3). Hence, the classical description of turbulence being induced by the mean velocity shear is not appropriate in the interior, except for at some locations such as the equatorial undercurrent (Toole 1998). We can also rule out boundary-forced convection, common in the ocean mixed layer during night time when surface cooling produces a top-heavy surface layer (e.g., Anis and Moum 1992), as this is unable to penetrate very far. One possible mixing process is double diffusion, which is a result of the different molecular diffusivities of salt and heat. This may occur when the density stratification is stable, but one of either salinity or temperature is unstably distributed in the vertical, for example, warm, salty water overlying cold, fresher water.

A more likely candidate is the mechanical production of turbulence by interaction of internal waves (Munk and Wunsch 1998; Toole 1998). Internal waves permeate the continuously stratified ocean interior, and may enhance each other to a degree that they become unstable and "break"[20]. Alternatively, internal waves may break against a sloping bottom (e.g., Stigebrandt 1976), and the

water mixed near the bottom is then transported horizontally along the isopycnals. That oceanic interior mixing probably is concentrated near irregular bottom topography, and not evenly spread out in the abyssal basins, is supported by the measurements of, for example, Polzin et al. (1997). They found diapycnal[21] diffusivities above the smooth abyssal plains in the central Brazil Basin to be about 10^{-5} m^2 s^{-1}, one order of magnitude lower (i.e. approximately ten times lower) than what estimates indicate is required for maintaining the abyssal stratification (Munk and Wunsch 1998). However, over the Mid-Atlantic Ridge they deduced diffusivities 50 times higher. One reason for this enhancement could be reflection of internal waves against a sloping bottom, which for certain angles between the incident wave and the bottom will increase the internal wave energy densities locally. In addition, as discussed in the following paragraph, the rough oceanic ridges may be where internal waves are produced.

Energy sources

Whatever the detailed mechanisms, there must be some source of energy which gives rise to the internal waves which in turn produce turbulence and mixing. The only possible candidates are the wind and the tides (Munk and Wunsch 1998). The wind may produce mixing by, for example, generating large-scale flows which interact with the bottom topography, or by generating internal waves that radiate from the surface layers into the interior. The tide gives rise to oscillating flows in the oceans which also may interact with the bottom topography, producing radiating internal waves that in turn can produce mixing (e.g., Sjöberg and Stigebrandt 1992).

---

20. My intuitive picture of internal wave mixing in the ocean interior is like the sea surface, covered by waves that occasionally break and foam, producing intermittent, sporadic turbulence.

21. Diapycnal mixing means mixing across pycnoclines.

Parameterizations of interior mixing in fjords

Since most Reynolds-stress turbulence models calculate the mixing from the mean shear, and do not include internal wave motions, they will yield no mixing in the interior water masses. This is particularly true for the different types of TKE models. In Paper III I briefly review some of the more common methods of parameterizing interior mixing in fjords and in the ocean. These range from simply setting a constant "background" diffusivity (e.g., Gillibrand et al. 1995) to adding extra stratification-dependent shear to the production term P in the equations for k and ε (e.g., Mellor 1989). In between one finds various methods of setting lower bounds on the diffusivity as functions of N or the local gradient Richardson number[22] (e.g. Kantha and Clayson 1994; Stacey et al. 1995).

A common drawback of all these parameterizations is that they do not explicitly depend on the strength of the underlying forcing, that is the process supplying the energy to the internal wave field. Since this can vary from system to system, the parameterizations above will lack in universality. What we need is a way of determining the internal wave mixing as a function of the energy sources, the wind and the tide.

A theory for interior mixing in fjords

Stigebrandt (1976) suggested that the internal tide could force the deep basin mixing in stagnant sill fjords. The internal tide is a result of the interaction between the barotropic tidal flow over the sill and the sill topography. Depending on the stratification within the fjord, the oscillating sill flow gives rise to progressive internal waves of different modes, which have the same frequency as the tide. These waves may then break against the sloping bottom, or possibly produce internal wave instabilities in the fjord basin. The energy flux from the barotropic tide to the first mode of the internal tide, assuming a two-layer stratification[23], was estimated for several

22. Similar to Ri in the previous chapter, but calculated from the actual gradients of velocity and density.

23. See Stacey (1984) for calculations of the energy flux for higher modes in a Canadian fjord.

Norwegian fjords by Stigebrandt and Aure (1989). They then compared these estimates to the observed mixing in the fjord basins below sill level and found that about 5-6 % of the internal tide energy flux produced deep water mixing. In addition, Stigebrandt and Aure found that the diffusivity was proportional to $N^{-1.5}$, where

$$N \equiv \left(-\frac{g}{\rho_0} \frac{\partial}{\partial z} \bar{\rho} \right)^{1/2}$$

is the buoyancy frequency[24], a measure of the local strength of the stratification. If the water is homogeneous, $N = 0$. If the stratification is unstable, N is imaginary since the term within parentheses will be negative. The inverse proportionality implies that the weaker the stratification, the stronger the mixing. This agrees with the form for the turbulent diffusivity in the oceanic deep water due to internal waves suggested by Gargett (1984), namely

$$\nu_t' = a_0 N^{-1} , \qquad (19)$$

where ν_t' is the turbulent diffusivity of heat and salt. Gargett estimated the factor of proportionality a_0[25] for the oceanic internal wave field from measurements of the dissipation, whereas Stigebrandt and Aure showed that in fjords it can be calculated with reasonable accuracy from the internal tide energy flux and a weighted average of the buoyancy frequency N. In other words, the deep basin mixing was a function of the amplitude of the

24. This is the frequency a small water parcel would oscillate up and down with, if displaced from its equilibrium position in a stable stratification (neglecting friction). Below its equilibrium position the parcel will have positive buoyancy and be forced up, and above this position it will have negative buoyancy and will sink. The stronger the stratification the faster the oscillations (higher frequency).

25. This parameter indicates the magnitude of the energy flux which produces mixing.

tidal variations outside the fjord, the topography of the sill and the stratification inside the fjord.

An alternative approach

A problem with the formula presented in the previous paragraph is the singularity at $N = 0$. When the stratification becomes very weak, such that N approaches zero, a_0 is divided by an increasingly small number and ν_t' grows very large. When N equals zero ν_t' becomes infinite. I have been investigating Byfjorden, a small sill fjord in the innermost part of the Orust-Tjörn fjord system (see Section 2.2), which is stagnant for long periods of time during which the deep water becomes increasingly homogeneous. Applying the equation proposed by Stigebrandt and Aure (1989) yields much too high deep basin diffusivities, and an ad-hoc upper limit must be introduced.

At this stage I came to think of the following. If I can calculate the internal wave energy that produces mixing in the fashion of Stigebrandt (1976), why not simply add this energy to the TKE-equation in the k-ε model? However, there is one problem. Even if I can calculate the total amount of energy to be added to the TKE, how should this be distributed with depth? Intuitively, I thought it reasonable that the stronger the stratification, the more "favorable" the conditions for internal wave activity. If there is no stratification one cannot have any internal waves. Furthermore, the direction of energy propagation of an internal wave is a function of the stratification. The stronger the stratification, the more vertical the direction of energy propagation. Hence, I conjectured, an internal wave packet inside the pycnocline will encounter lower stratification in both the upward and downward direction, which will tend to turn the propagation direction away from the vertical and hence "trap" the wave packet in the area of strong stratification. On the other hand, the vertical component of energy propagation will be largest in the pycnocline. Nevertheless, since earlier work indicated that the diffusivity was a function of the buoyancy frequency, my IWE term would probably have to be the same.

My hypothesis was supported by the work of Gargett and Holloway (1984). They argued that one should not separate between "mean" (including wave) and "turbulent" motions[26]. Assuming a flux Richardson number R_f[27] much smaller than 1 — which is supported by the results of Stigebrandt and Aure (1989) and others — and that the turbulence is due to wavelike motions (with a gradient wave Richardson number of order 1, that is close to critical), Gargett and Holloway found that

$$\varepsilon \propto N^e . \qquad (20)$$

The exponent e is 1 for the case of internal waves of almost a single frequency (narrow-band), such as internal seiches in a closed basin or internal tides dominated by a single tidal component. In the broad-band case, such as the deep-ocean wave field with a large range of frequencies and magnitudes, e becomes 1.5[28]. Further assuming that R_f is independent of N, Gargett and Holloway showed that Equation (20) implies a diffusivity ν_t' proportional to N^{-1} or $N^{-0.5}$, respectively.

Now, if the dissipation of TKE due to internal waves varies as N^e, it does not seem unreasonable that the TKE itself varies as N^e. Hence, as described in Paper III, I came up with the following extra term to be added to the k-equation (15):

$$\xi = aN^e . \qquad (21)$$

---

26. This obviously contradicts the separation of scales assumed when making the Reynolds-stress decomposition, the basis of all Reynolds-stress modeling. Whether this has any implications for the proposed IWE-extended k-ε model is still unclear to me.

27. This parameter relates the work done against gravity (which is a loss of turbulent energy) to the turbulence produced by shear. A small value implies that a small fraction of the available energy produces mixing.

28. However, other models yield $e = 2$ for the oceanic (GM) wave spectrum, which implies that the diffusivity for density is independent of the stratification (see, e.g., Toole 1998).

Here, the expected value for e is 1, and the energy magnitude a is given by the condition

$$\int_{-H}^{0} \xi A dz = C\frac{F}{\rho_0}, \qquad (22)$$

where $A(z)$ is the area of the fjord basin at each depth level (the hypsography), H is the total depth, F is the energy flux to the internal tide and C is a constant of proportionality which decides how much of the energy flux is available for mixing. Hence, Equation (22) says that if you sum up the term ξ throughout the fjord basin, it should equal the fraction C of the energy flux from the surface tide to the internal tide.

In Paper III I show that this model produces quantitative results for the weak deep water mixing in two Scandinavian fjord that agree well with observations. I also find that C should be about 1 and that the buoyancy term G in the equation for ε is irrelevant, that is $c_{3\varepsilon}$ is zero.

Stability functions and the turbulent Prandtl-Schmidt number

There is one problem with the IWE-extended turbulence model above. It is sensitive to the formulation of the parameter c_μ in Equation (16), as well as the corresponding parameter c_μ' in the equation for the turbulent diffusivity,

$$\nu_t' = c_\mu' k^{1/2} l \,. \qquad (23)$$

This sensitivity is not unique to the IWE parameterization I have proposed, but is a general feature of eddy viscosity models. However, the effects are more pronounced in the weakly stratified interior, where small variations in the turbulence may have a very noticeable impact on the development of the stratification.

As discussed in detail in a recent, as yet unpublished, paper by Burchard and Bolding (2000), the parameters c_μ and c_μ' are complex, non-dimensional stability functions that contain the information on all the correlations of higher-order terms that have been modeled to achieve closure.

There are several different versions of these stability functions (e.g., Mellor and Yamada 1974; Launder 1975; Galperin et al. 1988; Kantha and Clayson 1994; Burchard and Baumert 1995), some of which are discussed in more detail in the following section and Paper IV. However, it has for a long time been common practice to set the stability function for the viscosity c_μ to a constant value (e.g., Rodi 1987), and then use an empirical function for the turbulent Prandtl-Schmidt number σ_t. This number is defined as the ratio between the turbulent diffusivity and the turbulent viscosity, that is

$$\sigma_t \equiv \frac{\nu_t}{\nu_t'} .$$

The Prandtl-Schmidt number will be different depending on whether ν_t' is the turbulent diffusivity of salt, heat, TKE or some other property. Equations (16) and (23) then yield

$$c_\mu' = \frac{c_\mu}{\sigma_t} . \tag{24}$$

If $\sigma_t = 1$ the turbulent diffusivity of the property in question will be the same as the turbulent viscosity. For the diffusivities of TKE and dissipation, the Prandtl-Schmidt numbers are set to constant values close to one (see, e.g., Burchard et al. 1998).

It is in general assumed that the turbulent diffusivity of salt is the same as that for heat, since advection of small water parcels by turbulence should mix heat the same way as it does salt. However, it appears that the turbulent diffusivity of salt and heat [henceforth referred to as simply the (turbulent) diffusivity] is smaller than the turbulent viscosity for stratified flows (see, e.g., Launder 1975). This could be explained by the presence of internal waves, since these can transfer momentum but not salt or heat. Different formulae for the stratification-dependence of σ_t have been proposed.

In Figure 9 some of these are plotted as functions of a dimensionless parameter, which I will refer to as the turbulent Richardson number Ri_t, defined as

$$Ri_t \equiv \frac{k^2}{\varepsilon^2} N^2 .$$

As can be seen in Figure 9, there are quite large differences between the alternative formulae. In Paper III I have used the formula of Munk and Anderson (1948), but with the gradient Richardson number

$$Ri_g = \frac{N^2}{\left(\frac{\partial U}{\partial z}\right)^2},$$

where U is the mean velocity field, replaced by Ri_t. The reason is that the extra IWE term ξ affects k, and hence Ri_t, but has little impact on Ri_g, since velocity shears will still be very small in the deep basin.

As pointed out by my colleague Lars Axell[29] this substitution is not formally correct. Assuming stationary, homogeneous turbulence it can be shown from equation (15) that

$$Ri_g = \frac{c_\mu c_\varepsilon Ri_t}{1 + \frac{c_\mu c_\varepsilon}{\sigma_t} Ri_t}, \qquad (25)$$

where equation (24) has been used. Since $c_\mu c_\varepsilon \sim 0.1$ [30] and $\sigma_t \sim 1$, or perhaps one magnitude larger (as will soon be discussed), Ri_g is actually at least one magnitude smaller than Ri_t. As Ri_t increases so does the difference. This means that my modified Munk-Anderson formula will produce much larger values for σ_t than the original version.

---

29. Unfortunately after the paper had been accepted for publication...

30. Rodi (1987) suggests the value 0.09.

It has been suggested that σ_t should vary in the range 0.6 to approximately 2, increasing with increasing stability (e.g., Launder 1975). In my simulations of turbulent diffusion in stagnant fjord basins much higher values than this were computed, the mean deep water values being about 40. Please note, however, that the formula of Baum and Caponi (1992) yields even higher σ_t-values, as can be clearly seen in Figure 9. Reducing σ_t by multiplying Ri_t by 0.09 in my modified Munk and Anderson formula, a reasonable approximation of equation (25), yielded too much deep water mixing and thus poorer agreement with observations. Now, it should be emphasized that the narrow range of values for σ_t cited above is primarily based on observations of shear-driven turbulence in boundary layers. So, what should the ratio between turbulent viscosity and diffusivity be in the case of internal wave mixing in the interior?

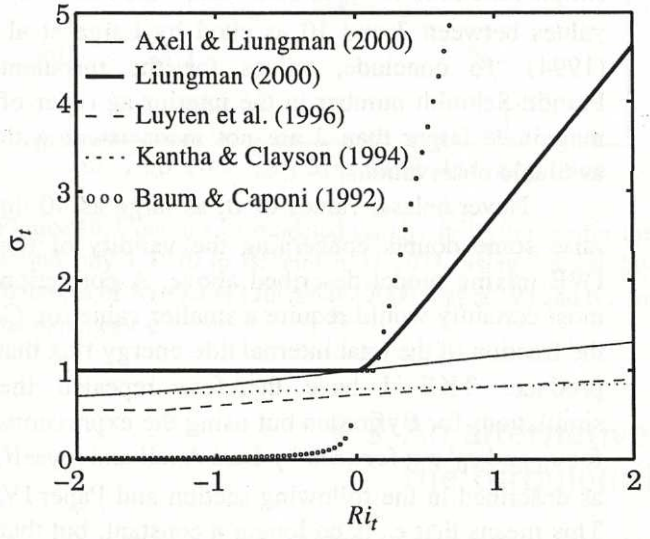

Figure 9. The turbulent Prandtl-Schmidt number σ_t as a function of Ri_t proposed by different authors. In some cases σ_t is not explicitly stated but has been deduced from the stability functions.

Large et al. (1994) set the Prandtl-Schmidt number for mixing generated by internal waves to 10, citing measurements by Peters et al. (1988). However, when presenting the method used to determine ν_t, the latter authors write: "If internal wave shear was important in production [of turbulence], ... [the equation yielding ν_t] is not justified." No "realistic" values for the turbulent flux of momentum were obtained in the core of the equatorial undercurrent, as the mean velocity shear

was negligible. Obviously, the method of Peters et al. could not resolve shear due to high-frequency internal waves, though their importance is acknowledged by the authors. Nevertheless, the *minimum* turbulent Prandtl number estimated from observations was 2, though not significantly different from 1 due to uncertainties in the measurements. Peters et al. also plotted empirical expressions for ν_t and ν_t', determined by fitting simple functions of Ri_g to their data, which show σ_t-values between 7 and 10 as cited by Large et al. (1994). To conclude, values for the turbulent Prandtl-Schmidt number in the interior an order of magnitude larger than 2 are not inconsistent with available observations.

Nevertheless, values of σ_t as large as 40 do raise some doubts concerning the validity of the IWE mixing model described above. A correction most certainly would require a smaller value for C, the fraction of the total internal tide energy flux that produces TKE. I have therefore repeated the simulations for Byfjorden but using the expressions for c_μ and c_μ' put forward by Lars Axell and myself, as described in the following section and Paper IV. This means that c_μ is no longer a constant, but that both stability functions, c_μ and c_μ', depend on Ri_t. The corresponding Prandtl-Schmidt number varies between 1.0 and 6.4 for stable stratification (see also Figure 9).

The simulated salinity stratification in Byfjorden for $C = 0.2$ is shown in Figure 10, to be compared with Figure 2 in Paper III. It is clear that a suitable adjustment of C will produce results just as good as those presented in Paper III, though no careful tuning has yet been performed. It is also interesting to note that the value 0.2 for C is the same as that commonly suggested for the mixing efficiency of deep water turbulence (e.g., Munk and Wunsch 1998). However, I would like to stress that CF is the fraction of the internal tide energy flux that becomes a source for TKE over the entire water column, not only the deep basin. Therefore, my

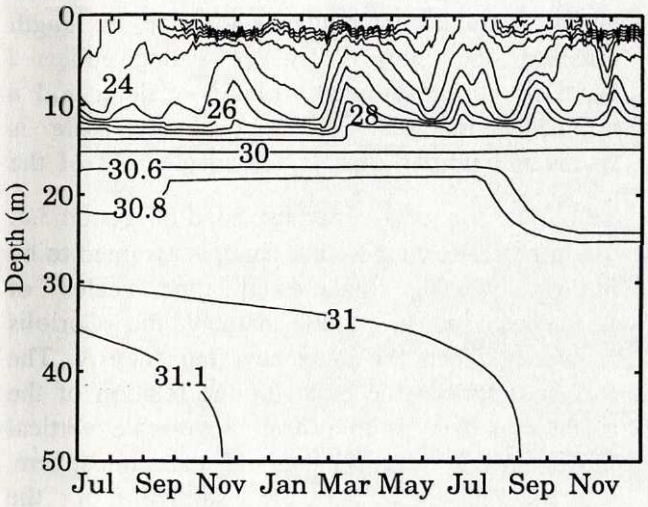

Figure 10. Contours of modeled salinity in Byfjorden for the period July 1 1970 to December 31 1971, using the stability functions of Axell and Liungman (2000; Paper IV) and 0.2 for the parameter C.

results need not contradict the findings of Stigebrandt and Aure (1989), discussed on page 53 in this section. Finally, it remains to be determined whether the modifications presented here will affect the already published results concerning the buoyancy term G in the ε-equation, and the corresponding value of $c_{3\varepsilon}$.

3.3 An alternative formulation of the turbulent length scale l

The final paper of this thesis deals with a one-equation k-l turbulence model, initially suggested by my colleague and co-author Lars Axell. Being displeased with the lack of an intuitive physical interpretation of the transport equation for ε, equation (18), he presented a simplified one-equation model where only the transport equation for k was retained, and the turbulent master length scale l was calculated from algebraic expressions. I was intrigued and tried his model on my fjord data, extending it with my IWE term. The results were identical to those of the k-ε model. After some discussions I managed to convince Lars Axell that we should write a quick, short note on this model. Of course, science is never that easy. After more than a year and three major revisions of the manuscript, our findings are now presented in Paper IV.

Hypothesis

The fundamental idea relies on the assumption that far away from the boundaries the size, or length scale, of the energetically dominating eddies l depends on the turbulent velocity scale q and a turbulent time scale t. The velocity scale is considered proportional to the square root of the TKE, that is $q \propto k^{1/2}$, as discussed in section 3.1. The time scale, on the other hand, is assumed to be limited by the fundamental time scales of geophysical mean flows, namely the Coriolis frequency f and the buoyancy frequency N. The former describes the effect of the rotation of the earth, which tends to restrict large-scale vertical movements in the oceans and the atmosphere, whereas N describes the strength of the stratification, which we already know will hinder turbulence. Since $k^{1/2}$ has the dimension m s^{-1} and f and N both have the dimension s^{-1}, it is clear that to get a length scale we must divide $k^{1/2}$ by either one of the two frequencies. Hence, the greater the frequency in question, the smaller the corresponding turbulent length scale. This is what we would expect. Near a boundary, on the other hand, it is reasonable to assume that it is the distance to this boundary which will determine how large the largest eddies can get, and hence l. Thus we have three possible length scales for the turbulent eddies.

Modeling

It has been shown again and again (see, e.g., Tennekes and Lumley 1972) that near a solid wall the velocity profile increases approximately logarithmically away from the wall[31]. Since the stress in this logarithmic layer is approximately constant, or at least scales as the wall stress, the eddy viscosity ν_t and thus the length scale will vary linearly with the distance d from the wall. Hence, near a wall

31. It should be mentioned that for ocean turbulence the surface is approximated as a solid wall.

$$l = l_g = \kappa d, \tag{26}$$

where κ is an empirical constant called von Karman's constant. We will call l_g the *geometric* length scale. Now, the rotation of the earth probably has very little effect on turbulent motions (see, e.g., Galperin et al. 1989), and we will therefore ignore this time scale. However, based on the buoyancy frequency N we define a *buoyancy* length scale

$$l_b = c_b \frac{k^{1/2}}{N}, \tag{27}$$

where c_b is another constant that needs to be determined. The buoyancy length scale will limit the turbulent length scale in cases of strong stratification far away from any wall.

To determine the master length scale l a first choice would be to say that it should be the smallest of the two length scales above. However, since it is not unreasonable to suppose that in some cases l could be affected by both proximity to a wall and stratification, we have assumed an expression of the form

$$\frac{1}{l^n} = \frac{1}{l_g^n} + \frac{1}{l_b^n}, \tag{28}$$

where n is some number greater than zero. If n is large, the smallest of l_g and l_b will dominate the value of l. In fact, if $n \to \infty$ we will get $l = \min(l_g, l_b)$. If $n = 1$ the result looks very much like the well-known Blackadar formula used by, amongst others, D'Alessio et al. (1998). We choose to set $n = 2$, because this gives equation (28) a number of desirable properties. In addition, our numerical experiments later showed this form to produce good agreement with measurements. Thus

$$\frac{1}{l^2} = \frac{1}{l_g^2} + \frac{N^2}{c_b^2 k}. \tag{29}$$

If there is no stratification ($N^2 = 0$) and l_g is generalized to include two walls, for example, surface and bottom, then we end up with a parabolic profile for l. Such a profile is in good agreement with laboratory measurements (e.g., Burchard et al. 1998). In a stable environment ($N^2 > 0$) far from a wall, that is l_g is large, l_b will limit the size of the turbulent eddies, which is what we would expect. What if the stratification is unstable, that is $N^2 < 0$? The last term in equation (29) will then be negative, which will increase l. This is also what we would expect, since convective overturning will increase the turbulent master length scale (see, e.g., McPhee 1994). However, if the buoyancy term becomes exactly the negative of the geometric term, they will cancel yielding zero. This requires an infinite value for l, which is obviously an unphysical result. To get around this problem we rewrite equation (29) as

$$l = l_g\left(1 - \frac{l^2}{l_b^2}\right)^{1/2}, \qquad (30)$$

where l on the right-hand side is the value calculated during the previous time step in the model. For negative values of l_b the turbulent master length scale l will become larger than the geometric length scale l_g, whereas $l_b \to 0 \Rightarrow l \to l_g$. To conclude, we use equation (29) when $N^2 \geq 0$ (stable or no stratification) and (30) when $N^2 < 0$ (unstable).

Stability functions revisited

The model is not complete until we have determined two things: the stability functions c_μ and c_μ', and the constant c_b. The latter will depend on the former. In the literature, a number of different stability functions have been suggested (e.g., Launder 1975; Galperin et al. 1988; Kantha and Clayson 1994; Luyten et al. 1996; see Figure 9). All of the above yield turbulent Prandtl-Schmidt numbers for neutral to strongly stable

stratification in the approximate range 0.7 to 1.5 (2.0 for Launder's versions). The stability functions of Galperin et al. and Kantha and Clayson do not exceed 1.05. Hence, all the proposed functions imply that salt and heat should mix more efficiently than momentum in the case of neutral flow (no stratification)[32]. In contrast, a recent review and compilation of measurements in the atmosphere by Högström (1996) suggests $1.0 \leq \sigma_t \leq 1.4$, that is all properties should be mixed to an equal degree by turbulent eddies when there is no stratification. Furthermore, the stability functions above produce a very modest increase in the Prandtl-Schmidt number for strong stable stratification.

To take into account these recent findings, Lars Axell and I decided to modify the coefficients in the stability functions of Launder (1975). The resulting expressions, which are functions of the turbulent Richardson number Ri_t, yield $\sigma_t = 1.0$ at neutral stratification and a limiting value of 6.4 as $Ri_t \to \infty$. Hence, our stability functions yield a larger difference between ν_t and ν_t' compared to other formulae (see Figure 9). However, in view of the discussion on deep water mixing in the previous section this may not be such a bad result. Furthermore, as shown in Paper IV this increase in the turbulent Prandtl-Schmidt number is required to match the empirical Monin-Obukhov similarity functions[33] of Högström (1996). This is further discussed below.

Finally, by simulating a Kato-Phillips type entrainment experiment and matching the model results to the algebraic solution of Price (1979) we find that 0.35 is an appropriate value for c_b.

---

32. Remember that the stability functions compute numbers which are multiplied with the product of the turbulent properties $k^{1/2}l$ to yield the eddy viscosity and diffusivity.

33. These functions describe how the heat and velocity gradients look in a near-wall shear layer experiencing a heat flux.

In Paper IV we compare this one-equation TKE-model to a number of laboratory and oceanic data sets, as well as the well-established model k-ε model. Since the parameter $c_{3\varepsilon}$ in the equation for ε also depends on the stability functions, we tuned this parameter in the same fashion as c_b. The results clearly show that the simplified k-l model performs just as well as the k-ε model.

Pros and cons

As we discuss in Paper IV several similar length-scale formulations have been proposed, though as far as we know none identical to ours. The advantages of our model compared to, for example, the k-ε or Mellor-Yamada models, is that only one transport equations needs to be solved and there is only one empirical parameter to be determined. We also expect this parameter c_b to be as universal as the different parameters in the ε-equation. When we set c_μ and c_μ' to constants, instead of functions of the stability, the tuned value of c_b only changed to 0.30. Furthermore, the formulation of the turbulent master length scale l appeals to our physical intuition. It is much easier to discern what happens in the model, as there is only one differential equation. Of course, this simple model cannot be expected to produce perfect results in all situations. However, I believe the major problem is probably the inaccuracy of the underlying concept, namely the eddy viscosity/diffusivity approach. As shown in Paper IV our model agrees very well with the empirical Monin-Obukhov similarity functions — as presented by Högström (1996) — which is considered an important test of any boundary layer turbulence model. Still the model overestimates the surface temperature at Ocean Weather Station Papa in the Northern Pacific Ocean (which of course could be due to poor parameterizations of the cross-surface heat fluxes). This may be considered an indication that the Monin-Obukhov functions, primarily determined from atmospheric measurements, are not such a suitable test for an ocean mixed layer model. The thickness of the surface layer in the atmosphere is of the order 10 to 100 m. Because of the difference in properties

between air and water, this is dynamically equivalent to only a few meters in the ocean. Now, the upper few meters in the ocean are affected by waves, Langmuir circulation, nightly convection, etc. Hence, to fine-tune the different constants in an eddy viscosity model, in order to match laboratory measurements or observations in the atmospheric surface layer, is perhaps not the best avenue of research if one is interested in modeling the ocean mixed layer[34].

Though a crude approximation, eddy viscosity models based on TKE-budgeting may still be useful, for the simple reason that they budget the energy available for mixing. What is needed are quantitative parameterizations of the energy input from processes that are currently not resolved or included, for example, convection, internal wave mixing, Langmuir circulation and perhaps most important mixing at and just below the pycnocline (see, e.g., Kantha and Clayson 1994; D'Alessio et al. 1998). In short, if we need to use a crude model, let us at least make sure that it includes the important processes, albeit in some simple fashion.

A final comment

In the, as yet, unpublished paper by Burchard and Bolding mentioned earlier, the authors discuss the behavior of different stability functions in terms of the critical and steady-state gradient Richardson numbers, Ri_g^c and Ri_g^{st} respectively. The first number is the Ri_g-value for which turbulent mixing in the model stops, due to insufficient shear in relation to the stability of the stratification. The second number is the value the model settles at when it has reached a steady state, that is when there are no more changes with time. The newer, and supposedly better, stability functions cited by Burchard and Bolding produce more mixing as they have higher values for the critical gradient

34. However, note that an assumed similarity between the oceanic and the atmospheric boundary layers, implying a universality of the Monin-Obukhov similarity functions, is the basis of the rather successful KPP-model of Large et al. (1994) (see also Large 1998).

Richardson numbers, namely $Ri_g^c \approx 1$. In comparison, the stability functions of Kantha and Clayson (1994) yield $Ri_g^c \approx 0.2$, which means that if the stabilizing stratification quantified by N^2 is more than 20 % of the turbulence-generating velocity shear squared, turbulent mixing is suppressed completely. In our model $\nu_t' \to 0$ as $Ri_t \to \infty$, which is equivalent to $Ri_f^c \approx 0.26$. Using $Ri_g = \sigma_t Ri_f$[35] we find $Ri_g \approx 1.64$, which is high indeed. The main reason is that our σ_t reaches significantly higher values for strong stable stratification than most other models, in order to match the measurements reported by Högström (1996). According to the argument of Burchard and Bolding this should mean that our model will mix more than previous models. However, the high value for the turbulent Prandtl-Schmidt number means that even though momentum may be efficiently mixed even if N^2 and the velocity shear squared are approximately equal, the same is not true for mixing of heat and salt. It can be shown that the steady-state gradient Richardson number Ri_g^{st} for our model is approximately 0.25, which agrees with the results of Burchard and Bolding. Please note that our value for Ri_g^{st} depends on the value of c_b, which was determined through the same calibration experiment as that used by Burchard and Bolding to determine Ri_g^{st}.

It is a bit confusing with all these different Richardson numbers. The flux Richardson number compares the shear generation and buoyancy destruction terms in the equation for TKE, whereas the gradient Richardson number compares the actual velocity and buoyancy gradients (shear and stratification). The turbulent Richardson number

35. This equality assumes that the turbulent diffusion of TKE and momentum are the same.

compares the buoyancy gradient to the ratio of TKE and dissipation. According to the scaling of Baum and Caponi (1992) this means that Ri_t is the ratio of the potential energy fluctuations associated with the turbulent motions, to the corresponding TKE. Hence, they claim this is a more "fundamental characterization" of the turbulence. It is not obvious to me which best describes the state of the turbulent environment.

It should be mentioned that Burchard and Bolding included the interior and pycnocline mixing parameterization of Large et al. (1994), which raises the question whether this could explain their good agreement between computed and observed surface temperature at OWS Papa. Again, we end up with the suspicion that important processes are missing in TKE mixed layer models.

4 Summary of papers

4.1 Paper I

In this paper — *Net circulation and salinity variations in an open-ended Swedish fjord system* — the subtidal circulation and salinity variations above sill level in the Orust-Tjörn fjord system are investigated by means of hydrographic observations and a process-oriented box model. This is motivated by the need for quantitative estimates of the exchange between the different fjord basins and between the fjord system and exterior water masses, which in turn are necessary when studying biogeochemical processes in, and human impact on, the fjord system. One main issue is to investigate a possible long-term, one-way net flow through the system indicated by earlier studies.

The basis for the investigation is the comprehensive monitoring program run by the Water Quality Association of the Bohus Coast since 1990 (BMP). The BMP data consists of monthly measurements of hydrography, nutrients and some biochemical parameters (see, e.g., Axelsson and Rydberg 1993), taken at a number of stations along the coast of Bohuslän in western Sweden. In addition, three smaller field programs were carried out between 1994 and 1996, aimed at investigating the water circulation in general and the net flow in particular with focus on the narrow straits in the northern parts of the fjord system: Malö Strömmar, Nordströmmarna and Nötesund (see Liungman et al. 1996).

The measurements indicate that on short time scales the current velocities in the narrow northern straits are dominated by the semi-diurnal tidal flow. However, ADCP measurements, as well as indirect measurements where the current in Malö Strömmar is inferred from the sea level difference over the strait, indicate a subtidal net flow with a variability

of a few days superimposed on variations with a time scale of 10 to 20 days.

The BMP data clearly show the influence of the exterior stratification on the hydrography inside the fjords. However, the exterior variations are gradually damped as they penetrate inside the fjord system. Furthermore, the average salinity for the years 1990 to 1996 at the northern entrance is about 2.4 psu higher than that outside the southern entrance to the fjord system. Occasionally this gradient reaches zero or reverses.

Calculating the steric height difference between the southern and northern entrances (Åstol and Byttelocket) yields an average difference of 2.8 cm. This agrees well with other estimates of the sea level slope along the Swedish west coast. Hence this is a prime candidate for driving a subtidal net flow through the system. A second, and perhaps more important, exchange process is the baroclinic flow associated with the adjustment of the water column inside the fjords to exterior variations in the salinity stratifications. Estimates of the exchange due to tides, local freshwater discharge and wind show that these are probably of minor importance in the long-term.

To test the steric height hypothesis a simple box model of the circulation above sill level in the Orust-Tjörn fjord system is implemented. The model divides the inner parts of the fjord system into two basins, where the southern basin (Havstensfjorden) consists of two boxes in the vertical and the northern basin (Koljöfjorden) of only one. The flow through the different constrictions (Nötesund and the Askerö straits), which may be multi-layered, is forced barotropically by the steric height difference (calculated from the observed salinity stratifications outside the two ends of the fjord system) and baroclinically by the density difference between the separate boxes. The model is tuned by comparing the upper layer salinities calculated by the model to those in the BMP data set.

The model is found to yield reasonable agreement between computed and observed

salinities. The larger errors appear to be due to variations in the exterior stratification not resolved in the BMP measurements. Comparison between modeled and observed net flow indicate that the model reproduces both the approximate magnitude of the net flow and the timing of reversals in the flow direction. For the simulated 7-year period the model computes a mean counterclockwise (mainly northward) transport of 72 $m^3 s^{-1}$. The subtidal net throughflow is in the counterclockwise direction 81 % of the time. Finally, numerical tracer experiments suggest that baroclinic flows through the southern entrance dominate the properties in the fjord, but that events with reversed net circulation may have a large impact on the northernmost fjord basin (Koljöfjorden). The estimated mean residence times for Koljöfjorden and Havstensfjorden are about 100 and 80 days, respectively.

4.2 Paper II

The paper entitled *Modeling and observations of deep water renewal and entrainment in a Swedish sill fjord* deals with a specific renewal event in the small Swedish sill fjord Byfjorden, located in the innermost parts of the Orust-Tjörn fjord system, during April and May 1974. Due to a field program being underway in Byfjorden at this time[1], a data set with relatively good temporal and spatial resolution is available. The main purpose is to investigate the effect of entrainment of resident water into the inflowing, juvenile water, a process often neglected when considering fjord renewals.

A one-dimensional model incorporating baroclinically and barotropically forced sill flow, entrainment of resident water into a descending gravity plume, and an extended TKE turbulence model, is implemented and used to investigate the

1. The reason for the field program was extensive dredging operations in the fjord.

effect of entrainment upon the post-renewal hydrographic state of the fjord. The results are compared to observed stratification and estimates of sill and entrainment flows based on data. Different entrainment parameterizations are tested and compared to each other as well as to data.

Observations indicate a consistent baroclinic inflow that is modulated by a semi-diurnal tidal flow. The sill flow is often two-layered, though there does not appear to be an obvious hydraulic control. Budget estimates yield a mean sill inflow of about 100 $m^3 s^{-1}$ over the renewal period of some 16-17 days. Approximately 55 $m^3 s^{-1}$ appears to descend all the way to the deep basin, entraining on average 84 $m^3 s^{-1}$ of resident water before interleaving. Hence, even though the total deep water inflow is sufficient to exchange the entire basin volume below sill depth, the resulting post-renewal deep water salinity is significantly lower than that of the exterior water mass during the renewal period.

Model simulations confirm these results. Though yielding a somewhat smaller sill flow (71 $m^3 s^{-1}$) the modeled mean inflow to the deep basin is 42 $m^3 s^{-1}$ with a mean entrainment of 111 $m^3 s^{-1}$. The difference between simulated entrainment and that computed from observations is shown to primarily be caused by different estimates of the salinity of the juvenile water. Using the model computed values, the estimates from data yield 44 $m^3 s^{-1}$ and 96 $m^3 s^{-1}$ for the deep basin inflow and entrainment, respectively, which is in good agreement with modeled results.

If entrainment into the descending bottom plume is neglected, the model is unable to reproduce the observed post-renewal stratification. Of the three entrainment parameterizations tested, the popular formula proposed by Turner (1986) showed the poorest performance, as it yields no entrainment for subcritical flow, that is in the upper parts of the plume's path where the difference in

salinity between the plume and the resident water is largest.

The model simulations clearly indicate the importance of considering entrainment of resident water during renewals in fjords, not only to the post-renewal density stratification but also to the oxygen concentrations in the deep basin. Mixing between juvenile and resident water substantially increases the time it takes for the basin water to be completely flushed during a renewal. In Byfjorden simulations showed that about 20 % of the deep basin water mass consisted of old resident water by the end of the renewal. This implies that post-renewal densities are lower than those found outside the sill during the renewal. Thus, entrainment of and mixing with resident water may have an influence comparable to that of deep water diffusion in setting the time scale for subsequent renewals.

4.3 Paper III

The third paper upon which this dissertation is based, entitled *Tidally forced internal wave mixing in a k-ε model framework applied to fjord basins*, suggests a simple method for including the energy flux from the barotropic tide to the internal tide in fjords in a two-equation turbulence model. The purpose is to find a more universal approach to simulating the weak interior mixing during basin water stagnation in fjords.

The proposed extension of the k-ε model to include internal wave mixing in fjords originates in the work of Stigebrandt (1976) and Stigebrandt and Aure (1989). They showed that the work done against buoyancy forces in the deep basin below the halocline[2] could be linked to the energy flux F from the barotropic tide to progressive internal waves of tidal frequency. This internal tide is a result of the

2. Commonly located at or near the sill depth.

interaction of the tidally oscillating sill flow with the sill topography, and is a function of the tidal amplitude and frequency, the depth and cross-sectional area of the sill section, and the stratification inside the fjord.

In the proposed model, the energy flux to the internal tide is included as a source term in the transport equation for the turbulent kinetic energy (TKE). Following Gargett and Holloway (1984) the internal wave energy (IWE) term is formulated as proportional to N^e, where e is 1.0 or 1.5. The constant of proportionality is determined such that the integral of the IWE term over the entire basin volume equals the fraction C of F that produces TKE.

The proposed IWE-extended k-ε model is incorporated into a 1-D numerical fjord model and compared to observations in two Scandinavian fjords. Only the first mode is considered when calculating F. The results show good agreement between simulated and observed development in the basin-water stratification for $e = 1.0$ and $C = 1.0$. It is also found that the buoyancy term in the equation for the dissipation rate of TKE can be neglected[3].

4.4 Paper IV

The fourth and final paper — *A one-equation turbulence model for geophysical applications: comparison with data and the k-ε model* — presents a simplified turbulence model of the k-l type, and compares this to a number of laboratory and oceanic data sets, as well as the two-equation k-ε model.

Second-order turbulence closure models employing the eddy viscosity concept usually solve

3. See chapter 3, section 3.2 for a reevaluation of the model using an alternative expression for the turbulent Prandtl-Schmidt number.

a transport equation for the turbulent kinetic energy k. The two-equation k-ε model in addition solves a transport equation for the dissipation rate ε, from which the turbulent length scale l needed to estimate the eddy viscosity and diffusivity can be determined. The ε-equation is more empirical than the k-equation and the physical meaning of some of its terms are not evident. Hence, a one-equation model where l is calculated algebraically from relevant geophysical length and time scales is proposed.

Neglecting the effect of the rotation of the earth on the turbulent motions, l is determined from a combination of two length scales. The first is the geometric length scale

$$l_g = \kappa(d + z_0),$$

where κ is von Karman's constant, d is the distance from the boundary and z_0 is the roughness length of the boundary. The second is the buoyancy length scale

$$l_b = c_b \frac{k^{1/2}}{N},$$

where c_b is an empirical constant to be determined and N is the buoyancy frequency. The two length scales are combined through the formula

$$\frac{1}{l^2} = \frac{1}{l_g^2} + \frac{1}{l_b^2}.$$

This formula has the following desirable properties. In the case of neutral stratification, a slight generalization of l_g to include a second boundary yields a parabolic profile for l. Also, near a wall the logarithmic velocity profile is predicted. Furthermore, a stable stratification $(N^2 > 0)$ reduces l and hence decreases turbulence. In the case of unstable stratification $(N^2 < 0)$ l is increased, using a slight reformulation to avoid the singularity at $l_b^2 = -l_g^2$.

The proposed k-l model was calibrated and tested using the stability functions of Launder (1975), but with modified coefficients to better agree with recent results on the atmospheric surface layer. The calibration yielded $c_b = 0.35$ and $c_{3\varepsilon} = -1.1$ for the k-ε model. The value for c_b yields critical and steady-state flux Richardson numbers that agree with measurements and other models. The comparisons then showed that the k-l model performed as well as the k-ε model for all the tested data sets.

The following conclusions can be drawn. For geophysical applications it currently appears unnecessary to solve an extra transport equation for the dissipation rate. Secondly, though the proposed model yielded very good agreement with the Monin-Obukhov similarity functions, it still overestimated the surface temperature observed at OWS Papa. This raises the question whether the Monin-Obukhov functions, determined from atmospheric measurements, are really a relevant test for ocean mixed layer modeling. Finally, what is needed are parameterizations of the processes that are currently not included in or poorly described by eddy viscosity TKE closure models, in particular interior mixing by internal waves and instabilities at the base of the pycnocline, nighttime convection and near-surface wind effects.

5 Conclusions and future outlooks

As is usual in research, the work I have presented in this thesis leaves several matters unexplored and probably raised as many questions as it answered. Nevertheless, I feel there are some tentative conclusions that may be drawn on the basis of my results.

Fjord modeling

Firstly, it would appear that we have most of the tools necessary for quantitative modeling of fjords and fjord systems. There will of course always be special cases where the theories discussed in this thesis are not readily applicable, or where completely different processes are important. The biggest obstacle, however, is the need for long-term observations of the exterior conditions with high vertical and, even more important, temporal resolution. If we are to calculate the hydrographic and biochemical state of a fjord we require such boundary conditions, since many fjords are strongly influenced by the conditions in the coastal waters outside. Furthermore, as stressed in chapter 2, short-term changes in the boundary conditions — on the order of weeks or even days — may result in the renewal of a fjord basin.

Unfortunately it is much more difficult to measure in the ocean than on land, and hence much more expensive. What is needed are reliable, automatic instruments that may be placed under water for long periods of time. Development of such hardware is under way, and perhaps we will soon have the same flow of information from below the sea surface as we now have from satellites and automatic weather stations.

Turbulent mixing

My lasting impression of the little work I have done on turbulence and turbulence modeling, is that there are a number of fundamental issues left to resolve. As the quote in the beginning of chapter 3 stated, understanding turbulence is currently one of physics' greatest challenges. Though we appear to

have a reasonable understanding of turbulence in homogeneous fluids and can simulate such flows with good accuracy, the field of turbulence in stratified fluids is still very much unexplored territory. A deeper understanding probably requires some radically new ideas. However, in the short term I believe we can come a long way towards more accurate estimates of mixing in the sea by building on the concepts we already have, and in a pragmatic way add simplified descriptions of the processes that are not included in the current models. This was my approach when I decided to add an extra term for internal wave energy to the equation for the turbulent kinetic energy (see chapter 3 and Paper III). Meanwhile, sophisticated computer simulations and clever laboratory experiments may shed more light on the links between mixing, large-scale turbulence, stratification and wave motions.

Suggestions?

Though I find it difficult to come up with any brilliant suggestions for the future, there are some things I would have liked to do had I had the time.

First, to put together a more or less complete model for the Orust-Tjörn fjord system, including a biochemical model to describe local biological and chemical processes, both in the open water and on/in the bottom sediment. The physical part of the model will then serve to set the abiotic conditions for these local processes. The biochemical model may have to be rather crude, but I still think we have the tools for learning a great deal about the fjord system in this way, particularly with the data available from the on-going monitoring program. The model could then be used as a kind of numerical laboratory, in which we can perform different kinds of experiments. Such a model could also serve as a way of bringing together knowledge from the many different research projects currently underway in the fjord system, as well as the researches themselves. If the model proves successful in describing ecological changes in the fjords, it could then be used as a tool for decision-

makers when evaluating, for example, the environmental impact of human activities.

Secondly, the model I have proposed for deep basin mixing in fjords should be more thoroughly tested. I feel confident that there are other fjords, especially in North America, where measurements of sufficient quality, quantity and temporal resolution are available. However, it may need some digging and sifting. I actually began testing the model on the world oceans, following in the footsteps of Sjöberg and Stigebrandt (1992) and using the new results of my colleague Karin Gustafsson, but never completed the calculations. It would be interesting to test the model for a case where the source for the internal wave energy is not the tide, but some entirely different process. I know my colleague and co-author Lars Axell is thinking hard on deep water mixing in the tideless Baltic Sea, so we may soon hear more about this.

The end

Well, this is the end of this thesis, and of several years of work. The roller-coaster ride is over. It has had its ups and downs, but it was seldom boring. I am definitely in line for the next of life's unpredictable rides, clutching my ticket in nervous anticipation...

References

Allen, G. L., and J. H. Simpson, 1998: Deep water inflows to Upper Loch Linnhe. *Estuarine, Coastal and Shelf Science*, **47**, 487-498.

Andersson, L., and L. Rydberg, 1988: Exchange of water and nutrients between the Skagerrak and the Kattegat. *Estuarine, Coastal and Shelf Science*, **36**, 159-181.

Anis, A., and J. N. Moum, 1992: The superadiabatic surface layer of the ocean during convection. *Journal of Physical Oceanography*, **22**, 1221-1227.

Axelsson, R., and L. Rydberg, 1993: Utvärdering av Bohusläns kustvattenkontrollprogram för perioden 1990-92. Hydrografi och näringsämnen. Department of Oceanography, Report No. 19 (Red Series), Göteborg University, Göteborg, Sweden (in Swedish).

Baum, E., and E. A. Caponi, 1992: Modeling the effect of buoyancy on the evolution of geophysical boundary layers. *Journal of Geophysical Research*, **97**, 15513-15527.

Bo Pedersen, F., 1980: A monograph on turbulent entrainment and friction in two-layer stratified flow. Ph.D. dissertation, Series Paper 25, Institute of Hydrodynamics and Hydraulic Engineering, Technical University of Denmark.

Borenäs, K., and A. Wåhlin, 2000: Limitations of the streamtube model. *Deep-Sea Research*, **47**, 1333-1350.

Burchard, H., and H. Baumert, 1995: On the performance of a mixed layer model based on the k-ε turbulence closure. *Journal of Geophysical Research*, **100**, 8523-8540.

Burchard, H., and K. Bolding, 2000: The role of stability functions in eddy viscosity turbulence models. Submitted to *Journal of Physical Oceanography*.

Burchard, H., O. Petersen and T. P. Rippeth, 1998: Comparing the performance of the Mellor-Yamada and the k-ε two-equation turbulence models. *Journal of Geophysical Research*, **103**, 10543-10554.

Cannon, G. A., J. R. Holbrook, and D. J. Pashinski, 1990: Variations in the onset of bottom-water intrusions over the entrance sill of a fjord. *Estuaries*, **13**, 31-42.

Christodoulou, G. C., 1986: Interfacial mixing in stratified flows. *Journal of Hydraulic Research*, **24**, 77-92.

D'Alessio, S. J. D., K. Abdella, and N. A. McFarlane, 1998: A new second-order turbulence closure scheme for modeling the oceanic mixed layer. *Journal of Physical Oceanography*, **28**, 1624-1641.

Edwards, A., and D. J. Edelsten, 1977: Deep water renewal of Loch Etive: a three basin Scottish fjord. *Estuarine and Coastal Marine Science*, **5**, 575-595.

Edwards, A., D. J. Edelsten, M. A. Saunders, and S. O. Stanley, 1980: Renewal and entrainment in Loch Eil; a periodically ventilated Scottish fjord. *Fjord Oceanography*, H. J. Freeland, D. M. Farmer, and C. D. Levings (Eds.), Plenum Press, 523-530.

Ehlin, U., 1971: Oceanografiska förhållanden i fjordsystemet innanför Orust och Tjörn och avloppsutsläppen från de petrokemiska industrierna i Stenungsund. SMHI (Swedish Meteorological and Hydrological Institute) utlåtande till Västerbygdens vattendomstol. SMHI, Norrköping, Sweden (in Swedish).

Ekman, M., 1994: Deviation of mean sea level from the geoid in the transition area between the North Sea and the Baltic Sea. *Marine Geodesy*, **17**, 161-168.

Ellison, T. H., and J. S. Turner, 1959: Turbulent entrainment in stratified flows. *Journal of Fluid Mechanics*, 6, 423-448.

Farmer, D. M., and H. J. Freeland, 1983: The physical oceanography of fjords. *Progress in Oceanography*, **12**, 147-220.

Fernando, H. J. S., 1991: Turbulent mixing in stratified fluids. *Annual Review of Fluid Mechanics*, **23**, 455-493.

Gade, H. G., 1973: Deep water exchanges in a sill fjord: a stochastic process. *Journal of Physical Oceanography*, **3**, 213-219.

Gade, H. G., and A. Edwards, 1980: Deep water renewal in fjords. *Fjord Oceanography*, H. J. Freeland, D. M. Farmer, and C. D. Levings (Eds.), Plenum Press, 453-489.

Galperin, B., A. Rosati, L. H. Kantha, and G. L. Mellor, 1989: Modeling rotating stratified turbulent flows with application to oceanic mixed layers. *Journal of Physical Oceanography*, **18**, 901-916.

Galperin, B., L. H. Kantha, S. Hassid, and A. Rosati, 1988: A quasi-equilibrium turbulent energy model for geophysical flows. *Journal of the Atmospheric Sciences*, **45**, 55-62.

Gargett, A. E., 1984: Vertical eddy diffusivity in the ocean interior. *Journal of Marine Research*, **42**, 359-393.

Gargett, A. E., and G. Holloway, 1984: Dissipation and diffusion by internal wave breaking. *Journal of Marine Research*, **42**, 15-27.

Geyer, W. R., and G. A. Cannon, 1982: Sill processes related to deep water renewal in a fjord. *Journal of Geophysical Research*, **87**, 7985-7996.

Gillibrand, P. A., W. R. Turrell, and A. J. Elliot, 1995: Deep-water renewal in the upper basin of Loch Sunart, a Scottish fjord. *Journal of Physical Oceanography*, **25**, 1488-1503.

Gillibrand, P. A., W. R. Turrell, and A. J. Elliott, 1995: Deep-water renewal in the upper basin of Loch Sunart, a Scottish fjord. *Journal of Physical Oceanography*, **25**, 1488-1503.

Gustafsson, B., and A. Stigebrandt, 1996: Dynamics of the freshwater-influenced surface layers in the Skagerrak. *Journal of Sea Research*, **35**, 39-53.

Haamer, J., 1995: Phycotoxin and oceanographic studies in the development of the Swedish mussel farming industry. Ph.D. dissertation, No. A4, Department of Oceanography, Earth Sciences Centre, Göteborg University, Sweden.

Högström, U., 1996: Review of some basic characteristics of the atmospheric surface layer. *Boundary Layer Meteorology*, **78**, 215-246.

Kantha, L. H., and C. A. Clayson, 1994: An improved mixed layer model for geophysical applications. *Journal of Geophysical Research*, **99**, 25235-25266.

Kjerfve, B., and K. E. Magill, 1989: Geographic and hydrodynamic characteristics of shallow lagoons. *Marine Geology*, **88**, 187-199.

Kowalik, Z., and T. S. Murty, 1993: *Numerical modeling of ocean dynamics*. World Scientific, 481 pp.

Large, W. G., 1998: Modeling and parameterizing the ocean planetary boundary layer. *Ocean Modeling and Parameterization*, E. P. Chassignet and J. Verron (Eds.), Kluwer Academic Publishers, 81-120.

Large, W. G., J. C. McWilliams, and S. C. Doney, 1994: Oceanic vertical mixing: a review and a model with a nonlocal boundary layer parameterization. *Reviews of Geophysics*, **32**, 363-403.

Launder, B. E., 1975: On the effects of a gravitational field on the turbulent transport of heat and momentum. *Journal of Fluid Mechanics*, **67**, 569-581.

Liungman, O., L. Rydberg, and G. Björk, 1996: Data report on measurements of currents, sea levels and hydrography in the Orust-Tjörn fjord system. Report No. C5, Earth Sciences Centre, Göteborg University, Göteborg, Sweden, 105 pp.

Luyten, P. J., E. Deleersnijder, J. Ozer and K. G. Ruddick, 1996: Presentation of a family of turbulence closure models for stratified shallow water flows and preliminary application to the Rhine outflow region. *Continental Shelf Research*, **16**, 101-130.

Martin, P. J., 1985: Simulation of the mixed layer at OWS November and Papa with several models. *Journal of Geophysical Research*, **90**, 903-916.

McPhee, M. G., 1994: On the turbulent mixing length in the oceanic boundary layer. *Journal of Physical Oceanography*, **24**, 2014-2031.

Mellor, G. L., 1989: Retrospect on oceanic boundary layer modeling and second moment closure. *Parameterization of Small-Scale Processes, Proceedings of Aha Hulikoa Hawaiian Winter Workshop*, Honolulu, HI, University of Hawaii at Manoa, 251-272.

Mellor, G. L., and T. Yamada, 1974: A hierarchy of turbulence closure models for planetary boundary layers. *Journal of the Atmospheric Sciences*, **31**, 1791-1806.

Mellor, G. L., and T. Yamada, 1982: Development of a turbulence closure model for geophysical fluid problems. *Reviews of Geophysics*, **20**, 851-875.

Munk, W. H., and E. R. Anderson, 1948: Notes on a theory of the thermocline. *Journal of Marine Research*, **3**, 276-295.

Munk, W., and C. Wunsch, 1998: Abyssal recipes II: energetics of tidal and wind mixing. *Deep-Sea Research*, **45**, 1977-2010.

Peters, H., M. C. Gregg, and J. M. Toole, 1988: On the parameterization of equatorial turbulence. *Journal of Geophysical Research*, **93**, 1199-1218.

Polzin, K. L., J. M. Toole, J. R. Ledwell, and R. W. Schmitt, 1997: Spatial variability of turbulent mixing in the abyssal ocean. *Science*, **276**, 93-96.

Price, J. F., 1979: On the scaling of stress-driven entrainment experiments. *Journal of Fluid Mechanics*, **90**, 509-529.

Price, J. F., and J. Yang, 1998: Marginal sea overflows for climate simulations. *Ocean Modeling and Parameterization*, E. P. Chassignet and J. Verron (Eds.), Kluwer Academic Publishers, 155-170.

Price, J. F., and M. O'Neil Baringer, 1994: Outflows and deep water production by marginal seas. *Progress in Oceanography*, **33**, 161-200.

Revstedt, J., 1999: On the modelling of turbulent flow and mixing in stirred reactors. Ph.D. dissertation, Department of Heat and Power Engineering, Division of Fluid Mechanics, Lund Institute of Technology, Lund, Sweden.

Robinson, I. S., L. Warren, and J. F. Longbottom, 1983: Sea-level fluctuations in the Fleet, an English tidal lagoon. *Estuarine, Coastal and Shelf Science*, **16**, 651-668.

Rodhe, J., 1996: On the dynamics of the large-scale circulation of the Skagerrak. *Journal of Sea Research*, **35**, 9-21.

Rodi, W., 1987: Examples of calculation methods for flow and mixing in stratified fluids. *Journal of Geophysical Research*, **92**, 5305-5328.

Rydberg, L., J. Haamer and O. Liungman, 1996: Fluxes of water and nutrients within and into the Skagerrak. *Journal of Sea Research*, **35**, 23-38.

Sjöberg, B., and A. Stigebrandt, 1992: Computation of the geographical distribution of the energy flux to mixing processes via internal tides and the associated vertical circulation in the oceans. *Deep-Sea Research*, **39**, 269-291.

Speziale, C. G., 1991: Analytical methods for the development of Reynolds-stress closures in turbulence. *Annual Review of Fluid Mechanics*, **23**, 107-157.

Stacey, M. W., 1984: The interaction of tides with the sill of a tidally energetic inlet. *Journal of Physical Oceanography*, **14**, 1105-1117.

Stacey, M. W., S. Pond, and Z. P. Novak, 1995: A numerical model of the circulation in Knight Inlet, British Columbia, Canada. *Journal of Physical Oceanography*, **25**, 1037-1062.

Stigebrandt, A., 1976: Vertical diffusion driven by internal waves in a sill fjord. *Journal of Physical Oceanography*, **6**, 486-495.

Stigebrandt, A., 1980: Barotropic and baroclinic response of a semi-enclosed basin to barotropic forcing from the sea. *Fjord Oceanography*, H. J. Freeland, D. M. Farmer, and C. D. Levings (Eds.), Plenum Press, 141-164.

Stigebrandt, A., 1981: A mechanism governing the estuarine circulation in deep, strongly stratified fjords. *Estuarine, Coastal and Shelf Science*, **13**, 197-211.

Stigebrandt, A., 1984: The North Pacific: a global-scale estuary. *Journal of Physical Oceanography*, **14**, 464-470.

Stigebrandt, A., 1987: A model for the vertical circulation of the Baltic deep water. *Journal of Physical Oceanography*, **17**, 1772-1785.

Stigebrandt, A., 1990: On the response of the horizontal mean vertical density distribution in a fjord to low-frequency density fluctuations in the coastal water. *Tellus*, **42A**, 605-614.

Stigebrandt, A., and J. Aure, 1989: Vertical mixing in basin waters of fjords. *Journal of Physical Oceanography*, **19**, 917-926.

Sullivan, G. D., and E. J. List, 1994: On mixing and transport at a sheared density interface. *Journal of Fluid Mechanics*, **273**, 213-239.

Svensson, T., 1980: Water exchange and mixing in fjords. Mathematical models and field studies in the Byfjord. Ph.D. dissertation, Report Series A:7, Department of Hydraulics, Chalmers University of Technology, Göteborg, Sweden.

Svensson, U., 1978: A mathematical model for the seasonal thermocline. Ph.D. dissertation, Report No. 1002, Department of Water Research and Engineering, Lund Institute of Technology, Lund, Sweden.

Tennekes, H., and J. L. Lumley, 1972: A *first course in turbulence*. MIT Press, 300 pp.

Tomczak, M., and J. S. Godfrey, 1994: *Regional Oceanography: An Introduction*. Pergamon, 422 pp.

Toole, J. M., 1998: Turbulent mixing in the ocean: intensity, causes and consequences. *Ocean modeling and parameterization*, E. P. Chassignet and J. Verron (Eds.), Kluwer Academic Publishers, 171-190.

Turner, J. S., 1979: *Buoyancy effects in fluids*. Cambridge University Press, pp. 368.

Turner, J. S., 1986: Turbulent entrainment: The development of the entrainment assumption, and its application to geophysical flows. *Journal of Fluid Mechanics*, **173**, 431-471.

På grund av upphovsrättsliga skäl kan vissa ingående delarbeten ej publiceras här.
För en fullständig lista av ingående delarbeten, se avhandlingens början.

Due to copyright law limitations, certain papers may not be published here.
For a complete list of papers, see the beginning of the dissertation.

GÖTEBORGS UNIVERSITET

Earth Sciences Centre, Göteborg University, A

1. Tengberg, A. 1995. Desertification in northern Bukina Faso and central Tunisia.
2. Némethy, S. 1995. Molecular paleontological studies of shelled marine organisms and mammal bones.
3. Söderström, M. 1995. Geoinformation in agricultural planning and advisory work.
4. Haamer, J. 1995. Phycotoxin and oceanographic studies in the development of the Swedish mussel farming industry.
5. Lundberg, L. 1995. Some aspects of volume transportsand carbon fluxes in the northern North Atlantic.
6. Lång, L-O. 1995. Geological influences upon soil and groundwater acidification in southwestern Sweden.
7. Naidu, P.D. 1995. High-resolution studies of Asian quaternary monsoon climate and carbonate records from the equatorial Indian Ocean.
8. Mattsson, J. 1996. Oceanographic studies of transportsand oxygen conditions in the Öresund.
9. Årebäck, H. 1995. The Hakefjorden complex.
10. Plink, P. 1995. A sedimentologic and sequence stratigraphic approach to ice-marginal deltas, Swedish West Coast.
11. Lundqvist, L. 1996. 1.4 Ga mafic-felsic magmatism in southern Sweden.
12. Kling, J. 1996. Sorted circles and polygons in northern Sweden.
13. Lindblad, K. 1997. Near-source behavior of the Faroe Bank Channel deep-water plume.
14. Carlsson, M. 1997. Sea level and salinity variations in the Baltic Sea,
15. Berglund, J. 1997. Mid-proterozoic evolution in southwestern Sweden.
16. Engdahl, M. 1997. Clast lithology, provenance and weathering of quaternary deposits in Västergötland, Sweden.
17. Tullborg, E-L. 1997. Recognition of low-temperature processes in the Fennoscandian shield.
18. Ekman, S. 1997. Quaternary pollen biostratigraphy in the British sector of the central North Sea.
19. Broström, G. 1997. Interaction between mixed layer dynamics, gas exchange and biological production the oceanic surface layer with applications to the northern North Atlantic.
20. Stenvall, O. 1997. Stable isotopic ($\delta^{13}C$, $\delta^{18}O$) records through the Maastrichtian at Hemmor, NW Germany.
21. Loorents, K-J. 1997. Petrology, brittle structures and prospecting methods in the "Offerdalsskiffer" from the central part of the Caledonian allochton in the county of Jämtland, Sweden.
22. Lindkvist, L. 1997. Investigations of local climate variability in a mountainous area.
23. Gustafsson, B. 1997. Dynamics of the seas and straits between the Baltic and the North Seas.
24. Marek, R. 1997. The Hakefjord fault.
25. Cederbom, C. 1997. Fission track thermochronology applied to phanerozoic thermotectonic events in central and southern Sweden.
26. Kucera, M. 1997. Quantitative studies of morphological evolution and biogeographic patterns in Cretaceous and Tertiary foraminifera.
27. Andersson, T. 1997. Late quaternary stratigraphic and morphologic investigations in the poolepynten area, Prins Karls Forland, western Svalbard.
28. Wallinder, K. 1998. An integrated geophysical approach to the evaluation of quaternary stratigraphy and bedrock morphology in deep, sediment-filled valleys, south-west Sweden
29. Lepland, A. 1998. Sedimentary processes related todetrital and authigenic mineralogy of holocene sediments: Skagerrak and Baltic Sea.
30. Eilola, K. 1998. Oceanographic studies of the dynamics of freshwater, oxygen and nutrients in the Baltic Sea.
31. Klingberg, F. 1998. Foraminiferal stratigraphy and palaeoenvironmental conditions during late pleistocene and holocene in south-western Sweden.
32. Charisi, S. 1998. Chemical paleoceanographic studies of the eastern Mediterranean-Middle East and eastern North Atlantic regions in the early Paleogene and late Quaternary.
33. Plink Björklund, P. 1998. Sedimentary processes and sequence stratigraphy in Late Weichselian ice-marginal clastic bodies, Swedish west coast and in Eocene foreland basin fill, the Central Tertiary Basin, Spitsbergen.
34. Borne, K. 1998. Observational study of sea andlandbreeze on the Swedish West Coast with focus on an archipelago.
35. Andersson, M. 1998. Probing crustal structures in southwestern Scandinavia: Constraints from deep seismic and gravity observations.
36. Nicolescu, S. 1998. Scarn genesis at Ocna de Fier-Dognecea, south-west Romania.
37. Bäckström, D. L. 1998. Late quarternary paleoceanographic and paleoclimatic records from south-west of the Faeroe Islands, north-eastern Atlantic ocean.
38. Gustafsson, M. 1999. Marine aerosols in southern Sweden.
39. Haeger-Eugensson, M. 1999. Atmospheric stability and the interaction with local and meso-scale wind systems in an urban area.
40. Engström, L. 1999. Sedimentology of recent sediments from the Göta Älv estuary-Göteborg harbour, sw Sweden.
41. Pizarro, O. 1999. Low frequency fluctuations in the Eastern Boundary Current of South America: Remote and local forcing.
42. Karlsson, M. 1999. Local and micro climatological studies with emphasis on temperature variations and road slipperiness.
43. Upmanis, H. 1999. Influence of parks on local climate.
44. Andreasson, F. 1999. Gastropod intrashell chemical profiles ($\delta^{18}O$, $\delta^{13}C$, Mg/Ca, Sr/Ca) as indicators of Paleogene and recent environmental and climatic conditions.
45. Andersson, T. 1999. Late Quaternary palaeoenvironmental history of Prins Karls Forland, western Svalbard: glaciations, sea levels and climate.
46. Brack, K. 1999. Characterisation of facies and their relation to Holocene and recent sediment accumulation in the Göta älv estuary and archipelago.

Earth Sciences Centre, Göteborg University, A

47. Gustafsson, M. 2000. Recent and late Holocene development of the marine environment in three fjords on the Swedish west coast.
48. Loorents, K-J. 2000. Sedimentary characteristics, brittle structures and prospecting methods of the Flammet Quartzite - a feldspathic metasandstone in industrial use from the Offerdal Nappe, Swedish Caledonides.
49. Marek, R. 2000. Tectonic modelling of south west Scandinavia based on marine reflection seismic data.
50. Norrman, J. 2000. Road climatological studies with emphasis on winter road slipperiness.
51. Ostwald, M. 2000. Local protection of tropical dry natural forest, Orissa, India.
52. Postgård, U. 2000. Road climate variations related to weather and topography.
53. Johansson, M. 2000. The role of tectonics, structures and etch processes for the present relief in glaciated Precambrian basement rocks of SW Sweden.
54. Ovuka, M. 2000. Effects of soil erosion on nutrient status and soil productivity in the Central Highlands of Kenya.
55. Thompson, E. 2000. Paleocene chemical paleoceanography : global paleoproductivity and regional (North Sea) paleoclimate.
56. Liljebladh, B. 2000. Experimental studies of some physical oceanographic processes.
57. Bengtsson, H. 2000. Sediment transport, deposition and environmental interpretations in the Skagerrak and northern Kattegat: grain-size distribution, mineralogy and heavy metal content.
58. Scherstén, A. 2000. Mafic intrusions in SW Sweden : petrogenesis, geochronology, and crustal context.
59. Arneborg, L. 2000. Oceanographic studies of internal waves and diapycnal mixing.
60. Bäckström, D.L. 2000. Late quaternary paleoceanography and paleoclimate of the North Atlantic Ocean.
61. Liungman, O. 2000. Modelling fjord circulation and turbulent mixing.

ISSN 1400-3813

Kompendiet, Göteborg
2000